Instituto Nacional de Astrofísica, Optica y Electrónica.

Reporte Técnico

MICRO-OPTICAL COMPONENTS: APPLICATIONS

Gabriel Sagarzazu
Francisco-J Renero-C

Agosto 2004
Tonantzintla, Puebla

El reporte que tiene en sus manos ó en su computadora, es el resultado del entrenamiento (prácticas profesionales) de Gabriel Sagarzazu, asesorado por un servidor, siendo estudiante de la Ecole Supérieure d'Optique (SupOptique) en Francia. Este reporte es continuación del trabajo de caracterización de micro-componentes ópticos fabricaos en silicio, desarrollado por Eugénie Dalimier y Guillaume Lecamp (reporte disponible en la Biblioteca del Instituto).

Este reporte es ahora parte fundamental para interesados en aplicaciones de micro-componentes ópticos fabricados en silicio, que decidí ponerlo a disposición del publico en la Biblioteca del Instituto.

El reporte se encuentra en la forma original escrita por Gabriel Sagarzazu.

Atte.

Francisco Renero
INAOE
Óptica

Sta. Tonantzintla, Puebla a 12 de diciembre de 2007.

Micro-Optical Components : Applications

By Gabriel Sagarzazu

Directed by Dr Francisco Renero

August 2004

Acknowledgement

I would like to thank Armando and Manuel for their very precious help during this two-months work. I would like to thank Dr Wilfrido Calleja too for his advices and of course Dr Francisco Renero for his incredible welcoming and kindness.

Introduction

The importance of MEMS (and MOEMS) is undeniable nowadays. Indeed, an incredible number of applications are concerned by those components which size is less than 1 mm (portable telephone filters, motors, pumps, airbags, printing systems, sensors, telecommunications, barcode readers etc …). This success can be explained easily if we consider the size of these components but also their low cost, their precision, their robustness, their response time or their high-resonance-frequency which makes them insensitive to vibratory perturbations.

Micro-optical components in silicon have been fabricated at INAOE. Those components depend on the wavelength of use and can be used as mirrors or lenses. The goal of my study is to find and to realize applications using these components.
I have chosen to present my work in this report in 3 parts. First of all, I will make a description of the micromirrors fabricated at INAOE and most of all I will recall the fabrication techniques which are used. Then, I will give examples of recent applications which use MOEMS. The purpose is to choose one of these applications and try to realize it using the mirrors fabricated at INAOE : this is the last part of this work.

I. Micromirrors fabricated at INAOE

A) Description

We will use in this work two different types of micromirrors. On the one hand, we have the spherical and aspherical mirrors which are static ones and on the other hand, we have planar mirrors which are movable. It is important to underline that the fabrication techniques used to produce them are absolutely different. Indeed, we use bulk micromachining in order to fabricate spherical and aspherical mirrors while surface micromachining is the technique used for movable mirrors fabrication.
An exhaustive characterization of the aspherical mirrors has been made by Eugénie Dalimier and Guillaume Lecamp (Study on micromirrors, directed by Dr Francisco Renero, August 2002).

B) Fabrication

In this part, we will describe the two fabrication techniques we have noticed.

1. Spherical and Aspherical Micromirrors

- *Spherical micromirrors*

The fabrication of a spherical micromirror can be divided in three steps. Firstly, we have to put a mask on the layer of silicon. Secondly, we etch the silicon with the mask. This is an anisotropic etching and in this way, we can form an inverted pyramid. Finally, after we have etched all the mask, the etching will go on and the inverted pyramid will become little by little a spherical depression (and thus a spherical mirror). We will describe here all these different steps.

The first step is the making of the mask. The technique used is photolithography. As we can see on fig.1 we oxidize the silicon with hydrogen peroxide or nitric acid and in this way, we have a layer of SiO_2 on the substrate. Then, we add another layer : the photoresist. Finally, we add a photolithographic mask which is not fabricated at INAOE. Then, we expose our system to UV radiations (8-11sec). After this step the photoresist is developed and we can now etch the mask itself with fluorhydric acid (HF). The last step is the dissolution of the photoresist with acetone.

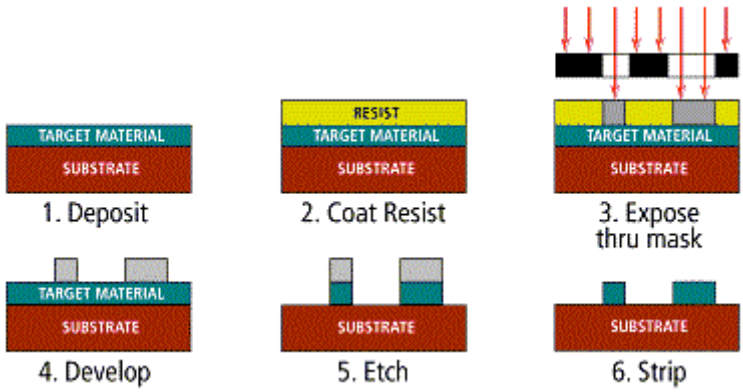

fig.1 : Photolithography

Once we have our mask of SiO_2, we can begin etching the substrate with KOH (hydroxide potassium). But in order to understand the fabrication of the micromirrors, we have to give some elements about the structure of silicon and about anisotropy. The silicon is a crystal and thus, we can observe it through different angles. In this way, we can distinguish different planes. We will consider for the moment only the planes 100, 110 and 111 (see fig.2). What's more, our silicon is Si 100 (it means that the surface of the substrate of Si is a 100 plane). If we have had an isotropic etching, the etch rate would have been the same for all the directions but here, the etch ratios of the different planes are different : the 110 plane is the fastest and the 111 is the slowest. This is not really surprising if we look at these planes (see fig.3). Indeed, the 110 plane is the least dense ; on the other hand, the 111 plane is the densest and that is why it is more difficult to etch this plane.

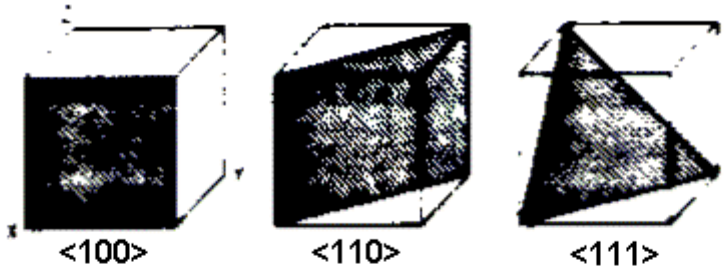

Fig.2 : Low crystalographic index planes of silicon

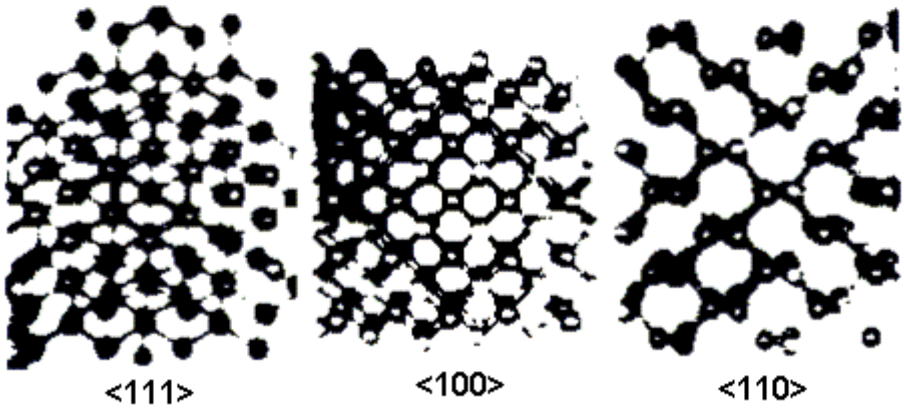

Fig.3 : Model showing three low-index directions of silicon

Thus, after having put a mask, we can etch the Si : this is the lithography with KOH and this etching is composed of two steps. First we form an inverted pyramid. We have said that the 111 plane is the slowest. Thus, all the "quick planes" will be etched until the 111 planes. Then the etching will be so slow that we can consider that this etching is stopped. We have formed in this way an inverted pyramid. We have to underline that the layer of SiO_2 is etched too and thus, we have to calculate the thickness of the mask because this layer of SiO_2 has to disappear after the formation of the inverted pyramid. The role of the mask is quite important here. Indeed, if the holes are square holes, the sides of the square have to follow the intersection between 111 and 100 (we avoid in this way undercutting). The pit depth is $do/\sqrt{2}$ where do is the diameter of the opening (see figure below).

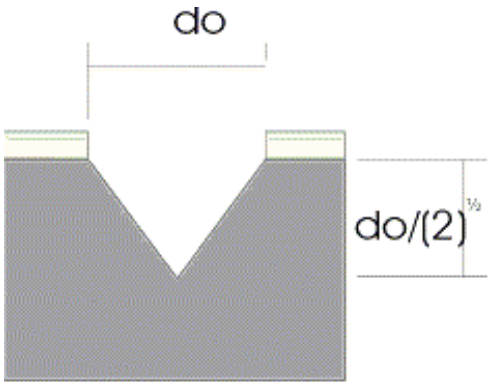

The last step is the formation of a spherical depression. The etching of the 411 planes is the fastest (faster than the 111 planes). Thus, another pyramid will be formed and will determine the sagitta :

$$s = do.\left[\frac{1}{\sqrt{2}} + \frac{1}{m}\left(\frac{1}{2}\sin\theta - \frac{1}{\sqrt{2}}\cos\theta\right)\right] \qquad (1)$$

Here, θ is the angle between the 411 and the 100 planes (θ = 19.47°). m is the etch ratio between these same two planes.
Then we will have a rounded surface :

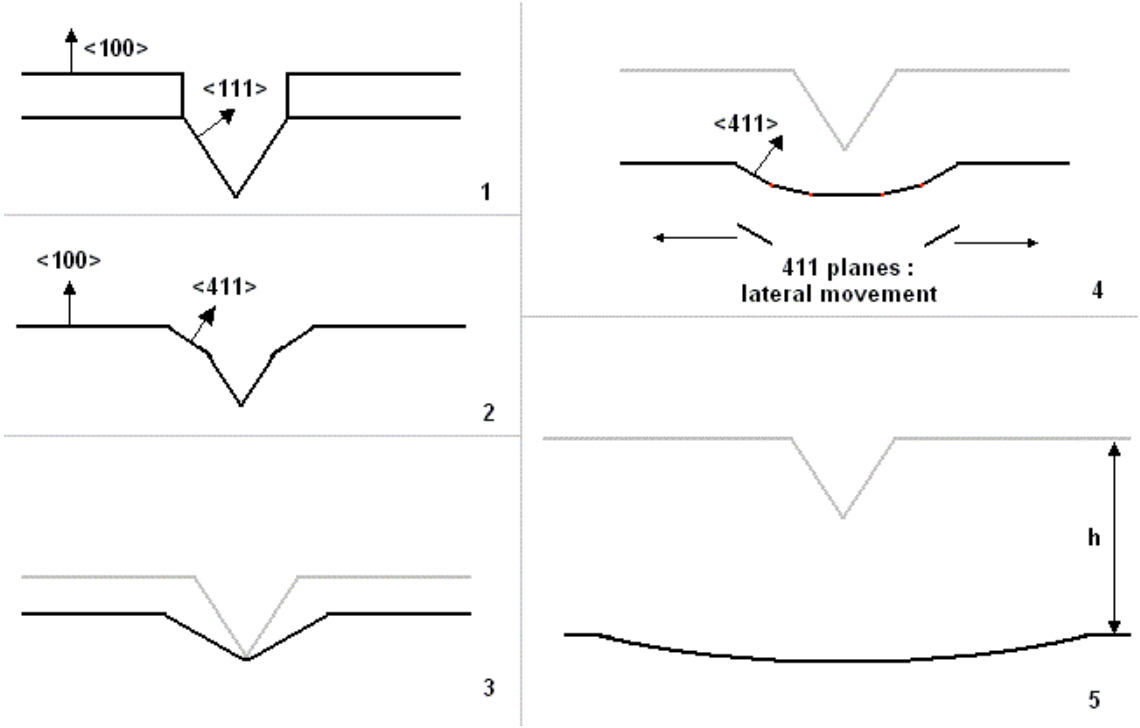

This is a consequence of the n11 planes which have a fast etch ratio. In this step, the 411 planes move laterally and they can go as far as disappearing if the etching lasts.
The diameter of the micromirror is given by :

$$D = 7{,}8.h^{0{,}58}.do^{0{,}42}$$

h is the etching depth (see the figure above). This is an empiric formula, conceptually valid for h > 2,5.do (at this depth, the 411 planes disappear).
We can give too the radius of curvature :

$$R_d = \frac{D^2}{8s} + \frac{s}{2}$$

Another important element is the normalised focal length :

$$\frac{f}{do} = 7{,}6\frac{\beta}{\alpha}\left(\frac{h}{do}\right)^{1;16}$$

where α is the expression inside brackets in (1) and β = 0,5 for a micromirror and β=1/(n-1) for a microlens.

- *Aspherical micromirrors*

Now we are able to fabricate spherical mirrors, we can focus on the aspherical mirrors. In fact, the idea is to superimpose spherical depression in order to approach an aspherical surface. Thus, we can make a model that is to say to use a set of balls with different diameters and the goal is to find the minimum approximation error of the surface (see fig.4).

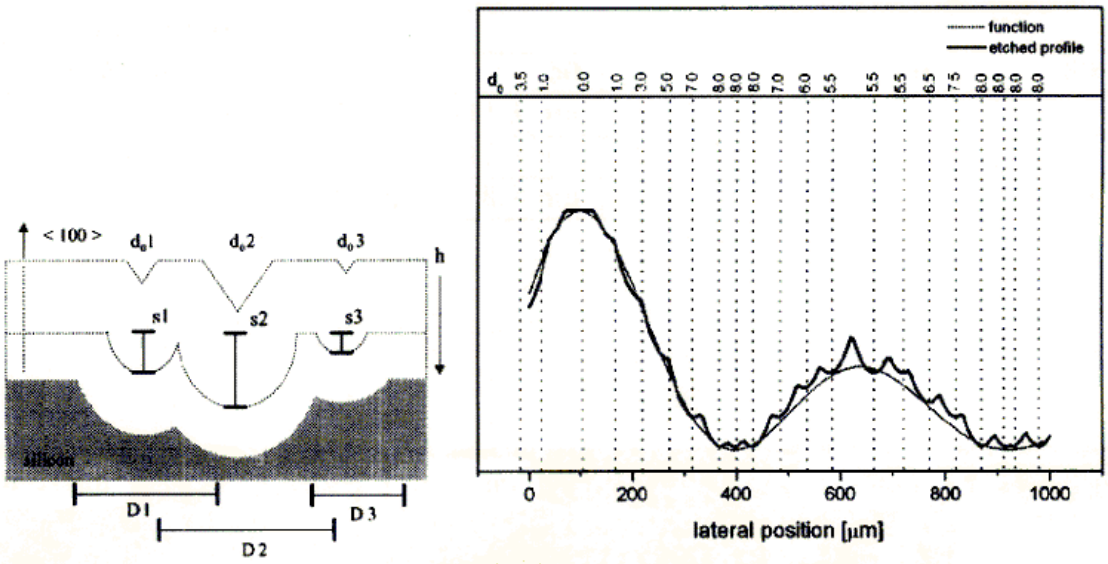

Fig. 4. Combined profile obtained from the lateral overlap of three spherical sections (left) and an arbitrary function approximated by an array of spherical depressions (right). The initial pit size is indicated at the end of line that represents the center of the respective depression.

If we have high spatial frequencies, the radius R_d must be small for a good approximation but if we want a smooth optical surface, this radius must be large !!

Thus, we have to find a compromise and in order to find this compromise we can modify :

- the grid pitch p
- the etch depth h
- the pit size do

We can give an example in fig.5 . The interferogram at the bottom right corner represents the interferogram of the aimed profile. If h is too small, we can see isolated cavities (h=20μm) but if h is too high, the interferogram will not be satisfactory (h=460μm for example). Here, h=150μm is the best fit.

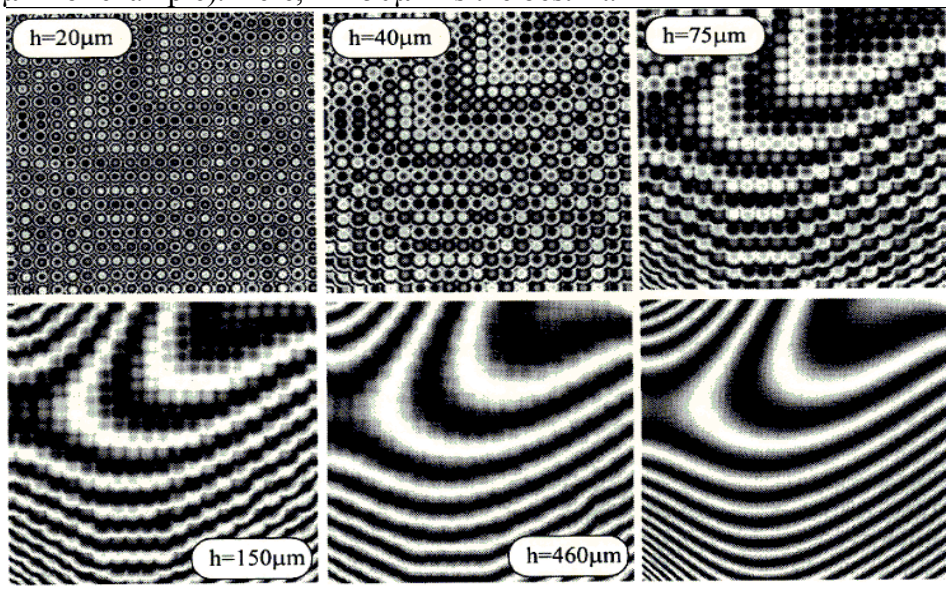

Fig. 5. Interferometric pattern of a grid of pits for various etch depths. The interferogram at the bottom-right corner represents the aimed profile.

There is a simple computer code which can give an approximative surface (and base of this “ball stamping” principle). Another approximation (in this code) is to consider that each spherical surface has only one common point with the real surface (thus, the error will be higher). First, the maximum of the function S(x,y) which represents the surface correspond to the sagitta and thus, we deduce the maximum pit size do_{max} and the etch depth h. Next, we calculate the other pits and the aimed profile is approximated by the lateral superposition of those depressions.

2. Surface Micromachining

We have described the anisotropic etching of Si with KOH which is bulk micromaching. The technique used to form movable micromirrors which is surface micromaching is absolutely different as we will see.

More precisely, the method used is polysilicon sacrificial surface micromachining. In this method, we do not etch the silicon itself but we will deposit different films on the silicon wafer and we will etch those films.
We can classify those films in two categories. On the one hand, we have structural materials which are typically polysilicon and on the other hand sacrificial material which is here an oxide (PSG).
The process can be divided in different steps. Each step is a disposition of a film or an etching of a layer deposited before. Each etching corresponds to a mask (a photoresist) we put above the wafer (there can be a contact between the mask and the previous layer but the photomask but it is not necessary). We have to distinguish negative photomasks and positive photomasks which belong to different results :

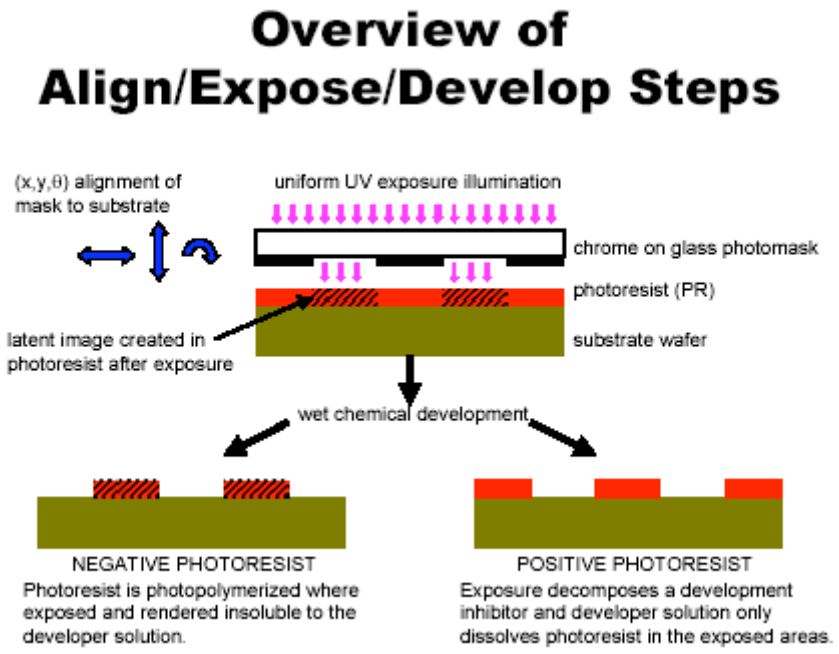

Concerning the deposits, we can distinguish planar deposit, conformal deposit and stacked deposit :

At each deposit, we have to precise the thickness of the layer. Of course, if we etch this layer later, the etch depth cannot be higher than this thickness.

In this way, we can obtain complicated structures if we use different layers of polysilicon (poly1, poly2, etc…).

At the end of the process, the sacrificial material (PSG) is wet etched away and thus, we obtain the final structure. In fact in our case, all the PSG is not removed.

The full process of our micromirrors will be described in part III.A

II. Recent applications or improvements

Nowadays, there are more and more applications which use micromirrors. In this part, we will give some examples. Of course, this presentation cannot be exhaustive and that is why I restricted myself to the field of the microscanners. The microscanners described here use surface micromachining but the movable micromirrors are quite different that the micromirrors fabricated at INAOE. Nevertheless, it can be interesting to analyse those micromirrors and to describe the different applications which use these components. Then, we will choose one application and we will try to make the same application using the micromirrors fabricated at INAOE.

A) Description of the microscanners

The applications I will describe use the same microscanners. Thus, it seems important to give a short description of this component.

The microscanners here are surface-micromachining electrostatic-com driven micromirrors. They have a high angular precision over a large scan angle.

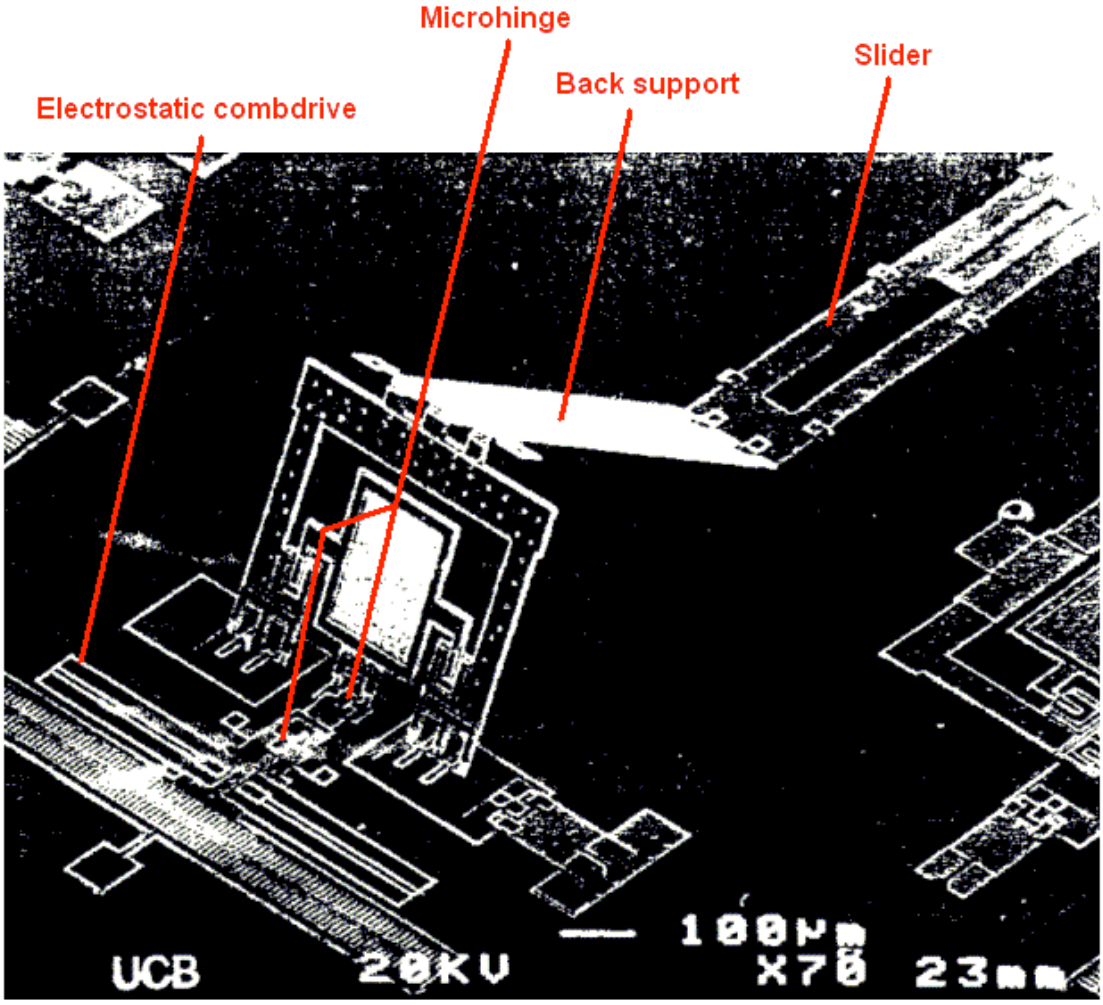

This mirror is compounded of different layers of polysilicon (see I.B.Surface Micromachining). The first one forms :

- the electrostatic combdrive
- the back support
- the slider
- the bottom plate of the hinge structure

The second one concerns :

- the pins in the hinges
- the guide for the slider

The third one concerns :

- the mirror
- the staples of the pins

The slider is moved only once during assembly and the combdrive allows the rotation of the mirror.
Thus here, the mirror is out of the plane and in this way, the propagation of the beams is parallel to the substrate.

This can use such a mirror in two different ways. On the one hand, it can be use as a galvanometric micromirror. In this case, it will produce steady state deflection with high fidelity. But it can be used as a resonant scanner too if it uses amplitude magnification.

B) Applications

We will present here 3 different applications using this kind of micromirror. Firstly, I will present a barcode reader that is to say a 1D-scanner. Then, I will describe two 2D-scanner : one which use two micromirrors and another which only use one micromirror.

1. Barcode Reader

This system is not really complex, we use here a resonant microscanner.
The principle is described in the figure below :

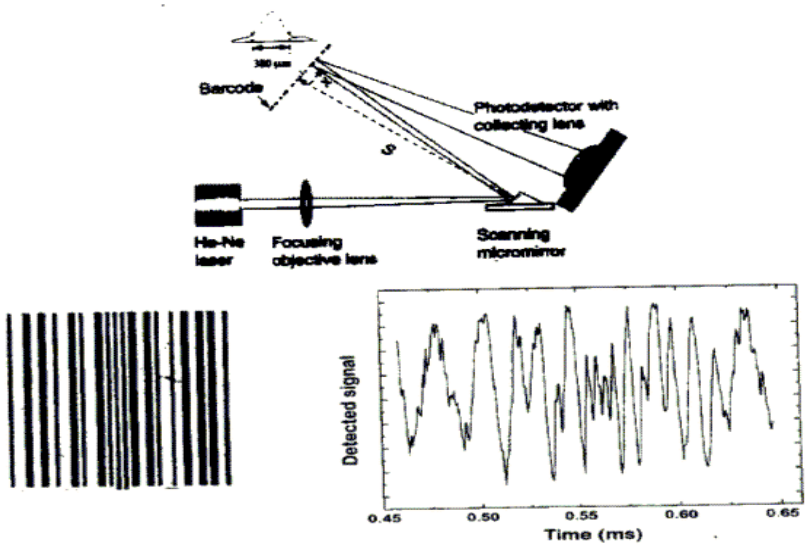

The scanning beam velocity varies in a sinusoidal fashion and we have to apply a mathematical transformation of the detected time signal :

$$X = S.\tan(\theta_s.\sin(\omega_o.t)$$

X represents the lateral displacement of the laser beam (relative to the center). S is the distance from the scanner mirror to the image plane. θ_s is the maximum excursion half-angle and ω_o is the angular resonance frequency.

The thinnest bars are 200µm bars. Here, we focus to 55µm on the mirror in order to avoid diffraction from the edges of the micromirror and 50mm after the mirror – that is to say at the plane of the barcode – the spot size is 190µm.

2. 2D-scanner using 2 movable micromirrors

A barcode reader could be fabricated using the micromirrors used at INAOE but a 2D-scanner must be more complex and most of all more interesting.

We can use for example two micromirrors in order to deviate a beam in two different directions. The first micromirror would be a resonant scanner and the second one a galvanometric scanner :

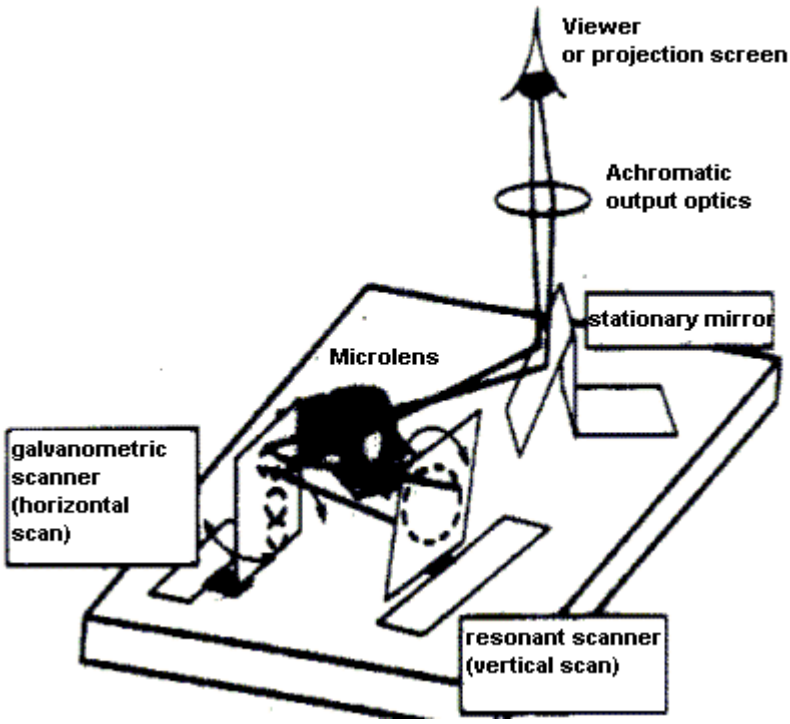

fig.6 : 2D microscanner with 2 micromirrors (and another stationary one)

The source here is a 3 color laser diodes or LEDs. The standard deviation is about 0,1% of the full scan and the quasi static angular deflection is quite good too :

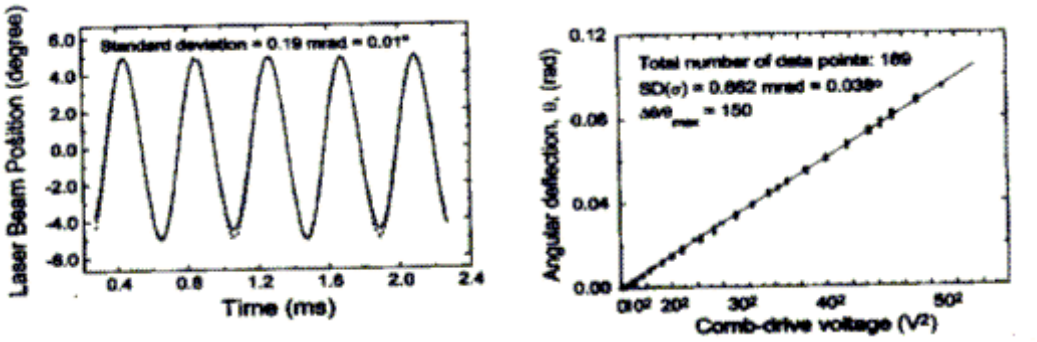

Here, the diameter of the mirror is 300µm.

3. 2D-scanner using 1 movable micromirror

It is possible to realise a 2D-scan using only one micromirror but we need a special source that is to say a fan laser.

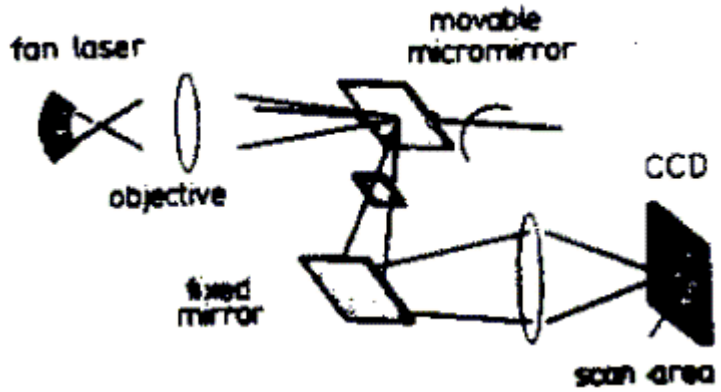

The fan laser is an array of light sources. The individual facets of the array are at discrete angles and thus, we can modify the beam direction in one dimension if we consider an angle or another.
The other dimension will concern the micromirror. The resolution in this direction is given by the divergence angle of the beam. Finally, this system has a resolution of 7X10 pixels.

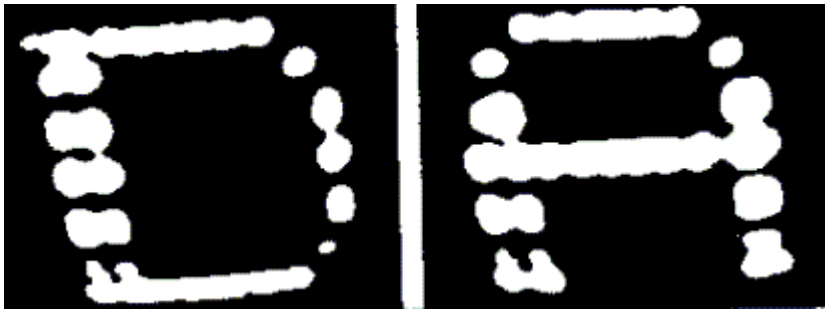

4. Conclusion

The last system could be interesting but the fan laser is a very special source. Thus, it may be more useful to work on a 2D-scanner which use 2 micromirrors.

Furthermore, we have not consider the static micromirror here. Nevertheless, the static micromirror is essential if we want to focus. Thus, a static micromirror after the two movable micromirrors is essential (see fig. 6).

III. Application : 2D-scanner

A) General description

The mirrors fabricated at INAOE and those which are described in part II are quite different. Thus, our scanner will be different. In this part, we will give a presentation of the system we will develop. More precisely, we will describe the general aspect of the movable micromirrors we will use (and thus we will see that they are very different if we compare them to the mirrors in part II). Then, we will give a sketch of our application in order to show how a 2D-scanner can be fabricated with INAOE micromirrors.

1. Movable micromirrors : description, process

We have seen that the fabrication technique is surface micromachining. We will give here an arbitrary example of movable micromirror ; we will describe it and insist on its process. The mirrors we will use will be different but the only difference will just concern the masks we will use. Indeed, the process will be exactly the same.

- *Description*

The figures below show an example of a movable micromirror we can fabricate at INAOE.

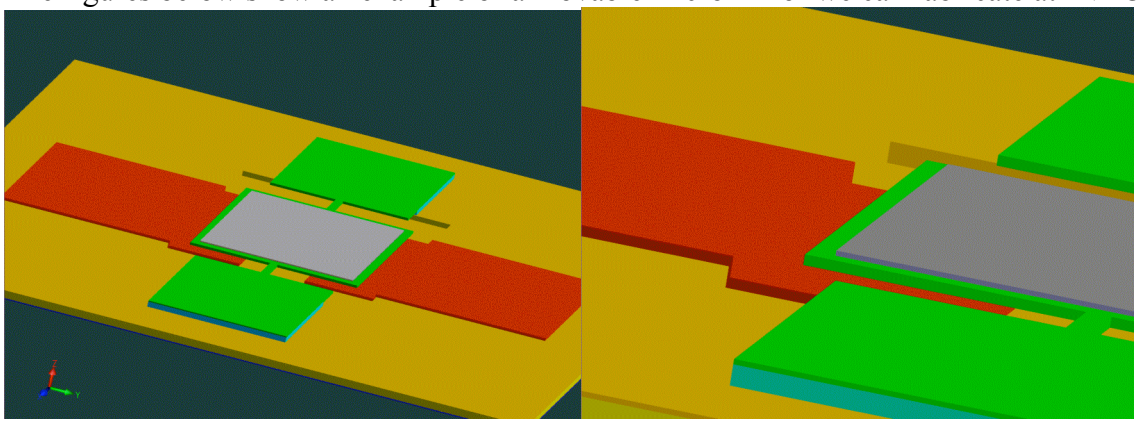

Thus, we can observe a well with two electrodes (poly1) inside. Just above, there is another layer of polysilicon (poly2) which can rotate around two narrow arms. Finally, we have a layer of aluminium on the poly2 : this is the mirror.
When we impose a voltage difference between one electrode and the poly 2, the two parts will approach : thus, the mirror rotate.

Here, the electric contacts are not represented.

- *Process*

We will give in this part a precise description of the process.
First, we have the substrate : a simple layer of Silicon (Si) with a layer of SiO_2 above :

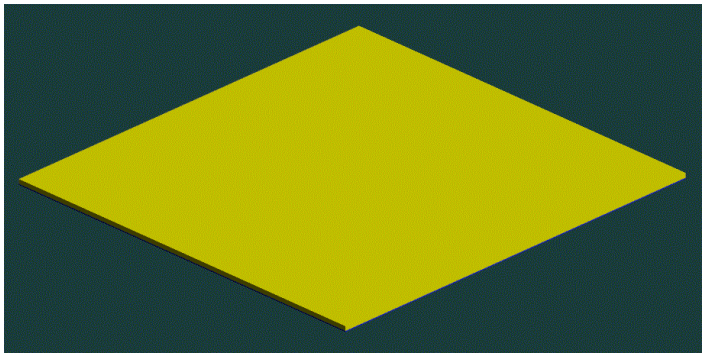

Then, we etch these layers and we oxidize :
The depth of the well is about 4µm (from 3 to 5µm).

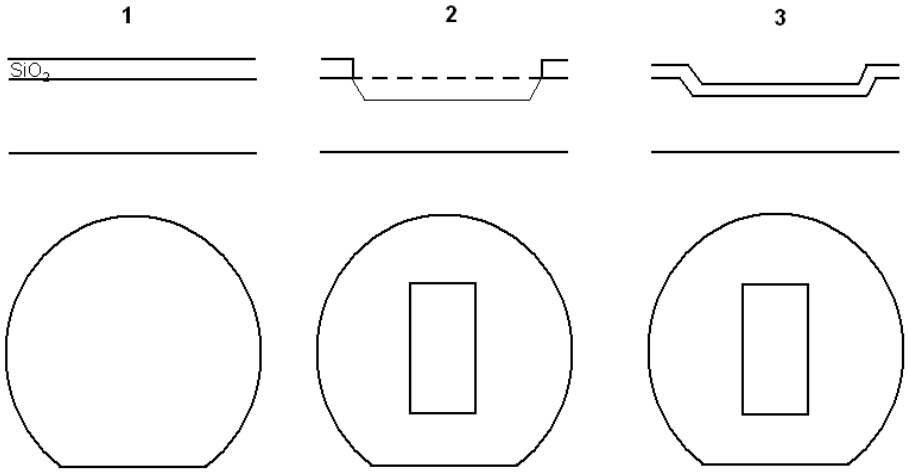

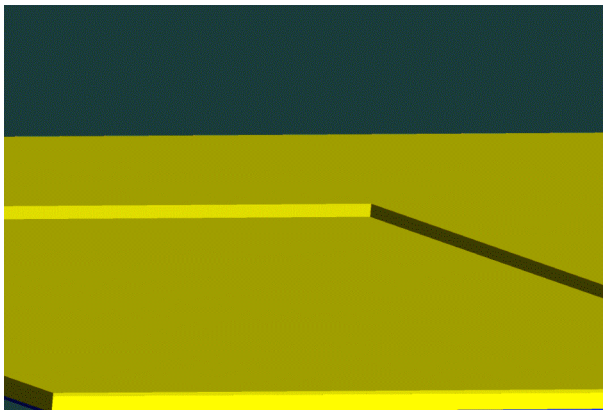

Then, we deposit a layer of poly1 (conformal deposit), we put a mask and we etch (positive etching) : we have formed the electrodes :

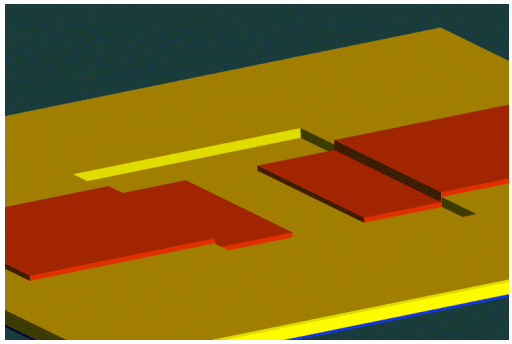

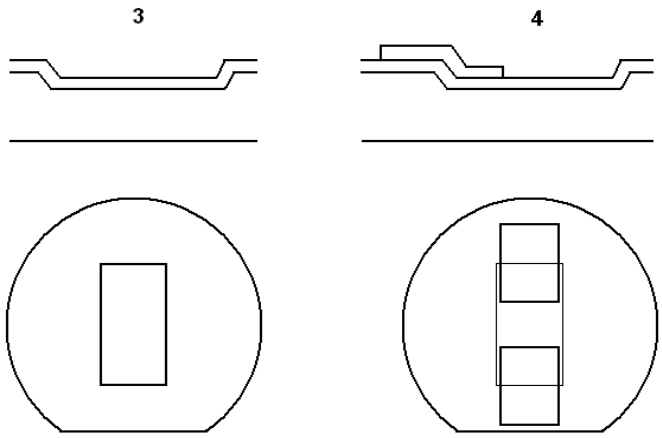

Then, we have to deposit the Poly2 but this layer must not touch the electrodes : we use here the PSG (stacked deposit).

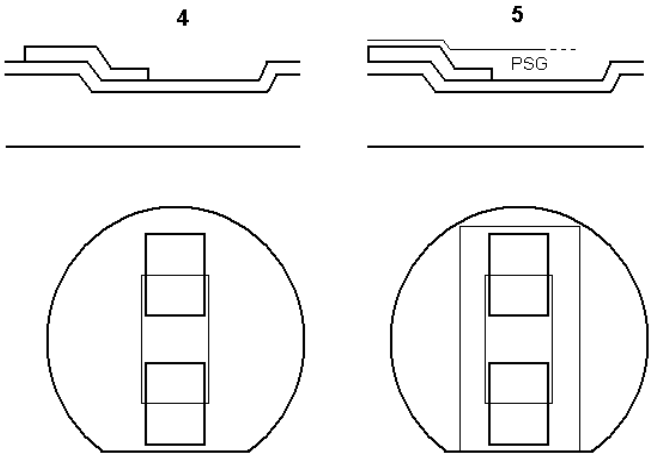

And then, we add a layer of Poly 2 and we etch it after having put a mask (positive etching)

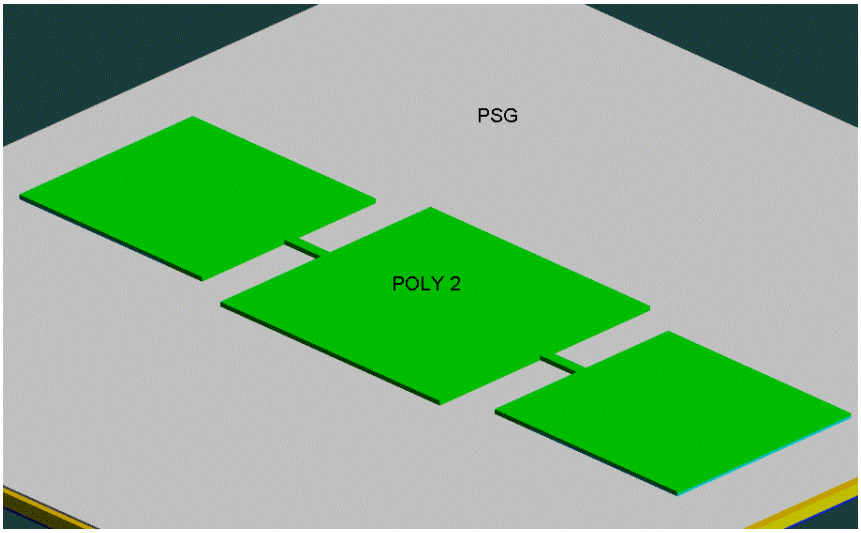

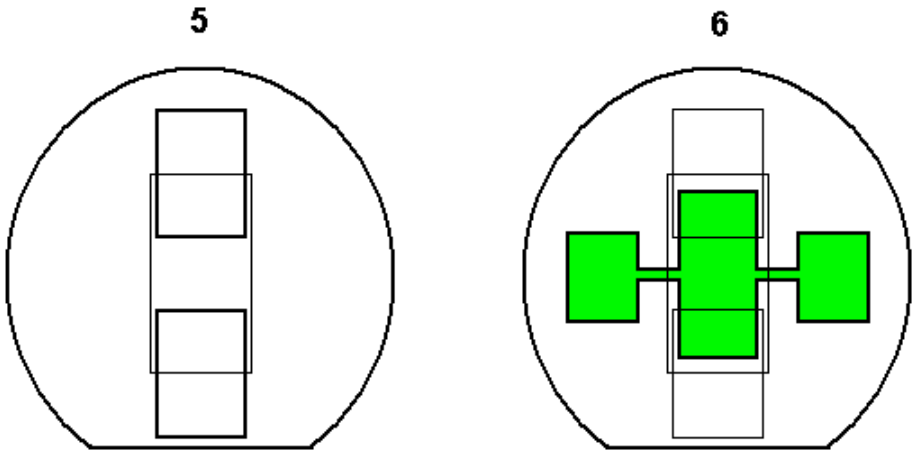

Then, we add a layer of aluminium and we etch. In reality, we put a layer of PSG between the poly2 and the layer of aluminium. In this way, the roughness of the mirror will be decrease.
Will do not represent the electric contacts here :

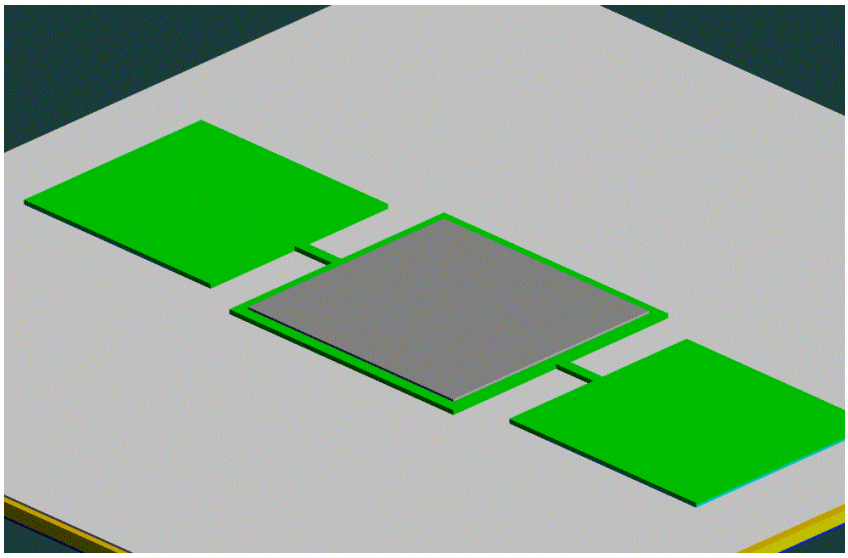

Finally, the PSG is removed (but not totally) :

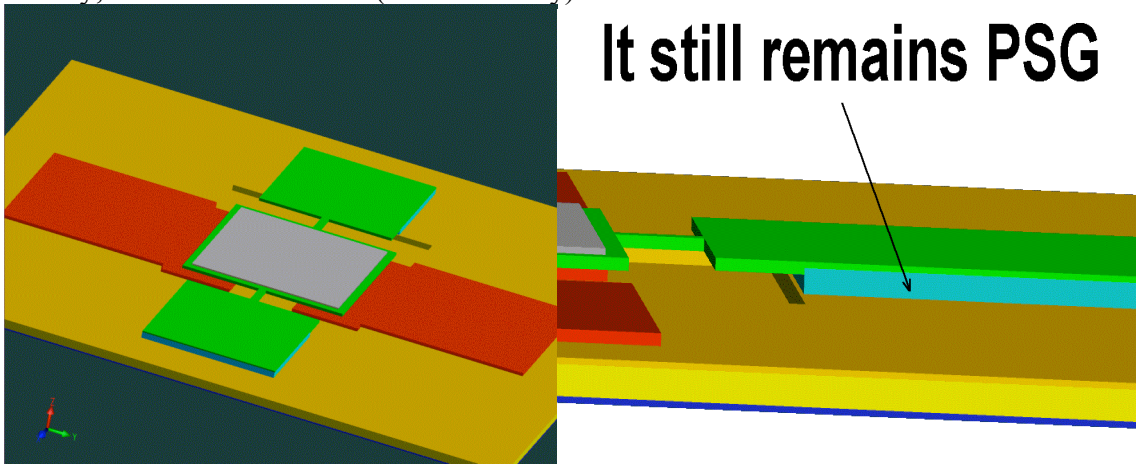

- *Electric contacts*

The contact will be made with a layer of aluminium. Here, the contacts have the form of a ring :

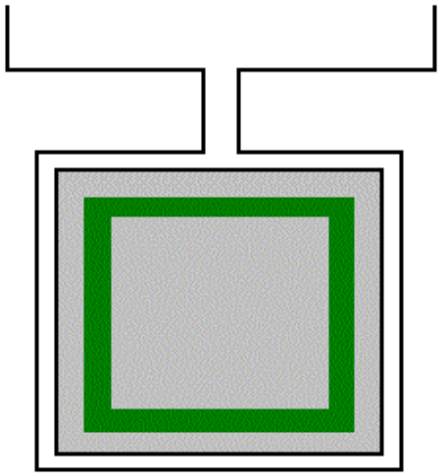

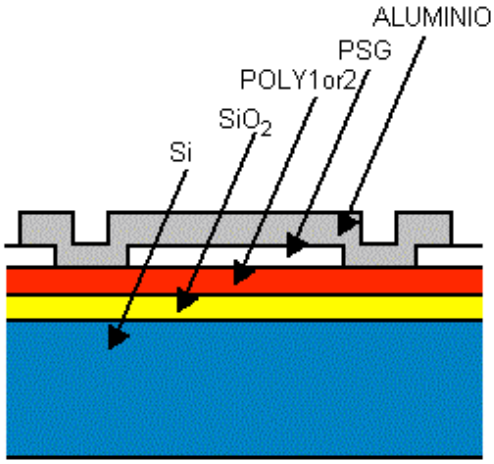

- *Commentary*

We have said that the size of the well is about 4µm. Thus, we cannot fabricate a movable aspherical micromirror because the sagitta measures 8µm (more or less) and it can be concluded that we need three mirrors in order to fabricate a 2D scanner (2 planar micromirrors and 1 aspherical).

2. First description of the scanner

We have seen in part II a scanner 2D and the propagation of the beam in this scanner was parallel to the substrate. This was a consequence of the back support which made the mirror raise. But in our case, the mirror is always parallel to the substrate and thus, we cannot have the same propagation of the beam.
A solution could be to fabricate the three micromirrors on different planes (and we would align those planes in a convenient way) but it seems difficult to align them perfectly (that is to say with a precision of some micrometers).
Another solution would be to put the three micromirrors on the same substrate and to add a planar mirror above. In this way, we do not have any problem of alignment. The figure below is an illustration of such a scanner (not yet optimized). This is an image from COVENTOR (see part III.C) which simulates the movement of the planar micromirrors but with this software concerns only surface micromachined systems and that is why the 3rd micromirror (the aspherical one) cannot be simulated. Nevertheless, we can represent it by a square in order to give a general idea of the system :

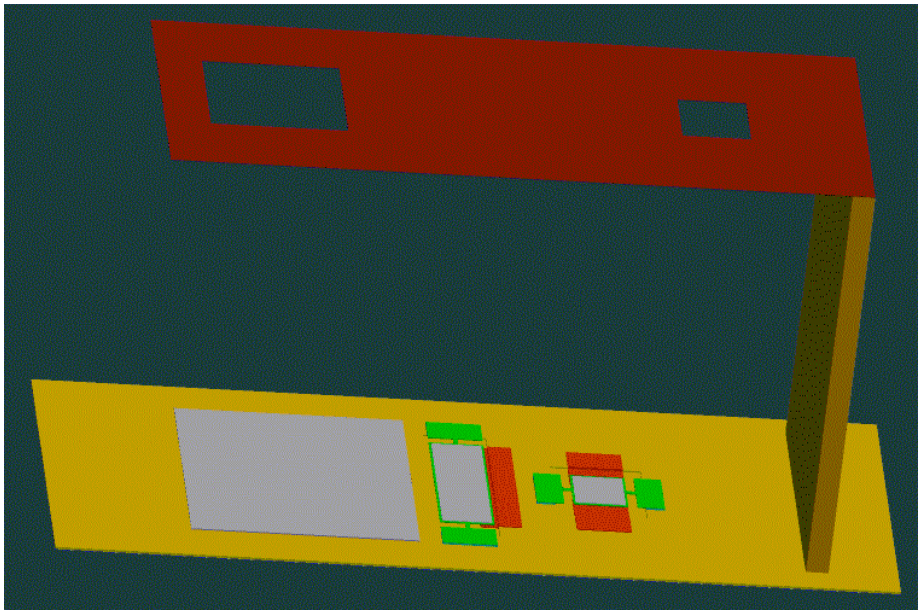

The light beam comes from the little window. Then, it is reflected by the first micromirror (resonant mirror), then the beam is reflected by the top (planar and static mirror). The galvanometric mirror makes a 3rd reflection. Then the beam is reflected by the top and comes to the aspherical micromirror which focuses the beam. Then the beam light can propagate and it will go through the 2nd window (larger than the first one).

We suppose in order to optimize our system that we will use a “traditional source” (that is to say we have not a laser). Furthermore, we suppose that the size of the beam at the beginning is 100µm (maximum). This beam would be collimated and thus, we have a planar wave-front until the beam reach the aspherical mirror.

We see here that the two planar micromirrors move around two different directions. Furthermore, the 2nd one has only one electrode : this electrode can attract the mirror but we will suppose that it can repulse it too (even if I did not succeeded in simulating this movement with COVENTOR).

B) Dimensions, characteristics of the system

In this part, we will explain how we will get the different dimensions of the system. First, I have chosen an arbitrary size for the aspherical micromirror that is to say 500-505µm. Indeed, the mirror has to be large enough in order to have a large optical scan and this figure corresponds to a large spherical micromirror (see Eugénie Dalimier and Guillaume Lecamp’s report).

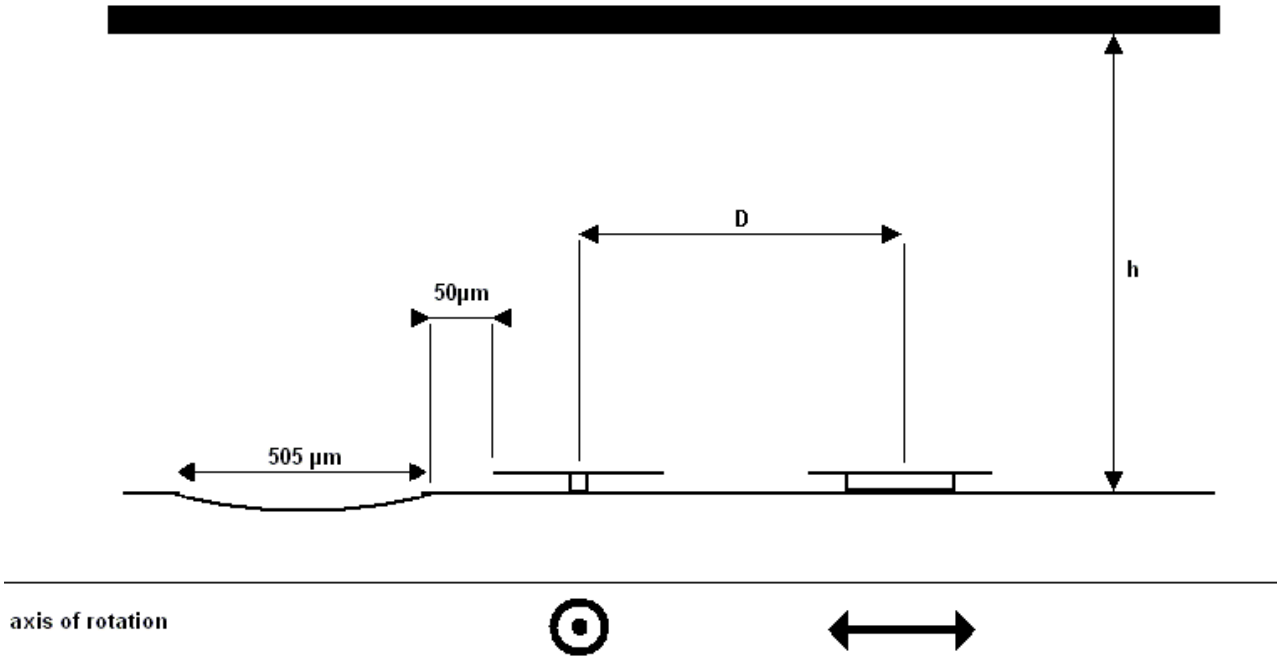

Furthermore, we consider that the distance between this mirror and the galvanometric one is about 50µm. We could imagine that we would fabricate the static micromirror and then, we would protect it and fabricate the 2 movable mirrors. Thus the distance between the static mirror and the galvanometric one has to be sufficient and 50µm seems to be reasonable.
The galvanometric mirror has only electrode because if we have had a second electrode, this mirror would have been further from the static one, thus the angle θ between the beam and the aspherical mirror would have been higher and thus, there would have been more aberrations (that is to say the resolution would have been worse).

Then, we will consider the distance h between the top of the system (the static planar mirror) and the back (the 3 micromirrors).
Indeed, this distance will be responsible of the total optical scan but it will be responsible of the resolution too. What's more, our mirrors cannot move indefinitely. Indeed, the movement is limited by the depth of the well. This is another limitation of the distance h : the more the mirror can move, the higher will be the possible maximum scan angle and the least will be the distance h (in order to have this great scan angle). These two limitations are independent and we will try to find a compromise between them.

1. The aberrations

We suppose here that the aberrations are the predominant limitation (and that we can move the mirrors indefinitely).

When the two first mirrors move, they deviate the beam and the incidence angle will vary but the spot size must not vary (the resolution must be the same). Thus, for different "maximum angles θmax" (for the beam, see the figure below), we will find the

best profile and finally, we will try to determine what is the most reasonable angle θmax. This angle will determine h and then we will deduce all the other dimensions.

Case : θmax : the resonant mirror has not moved.

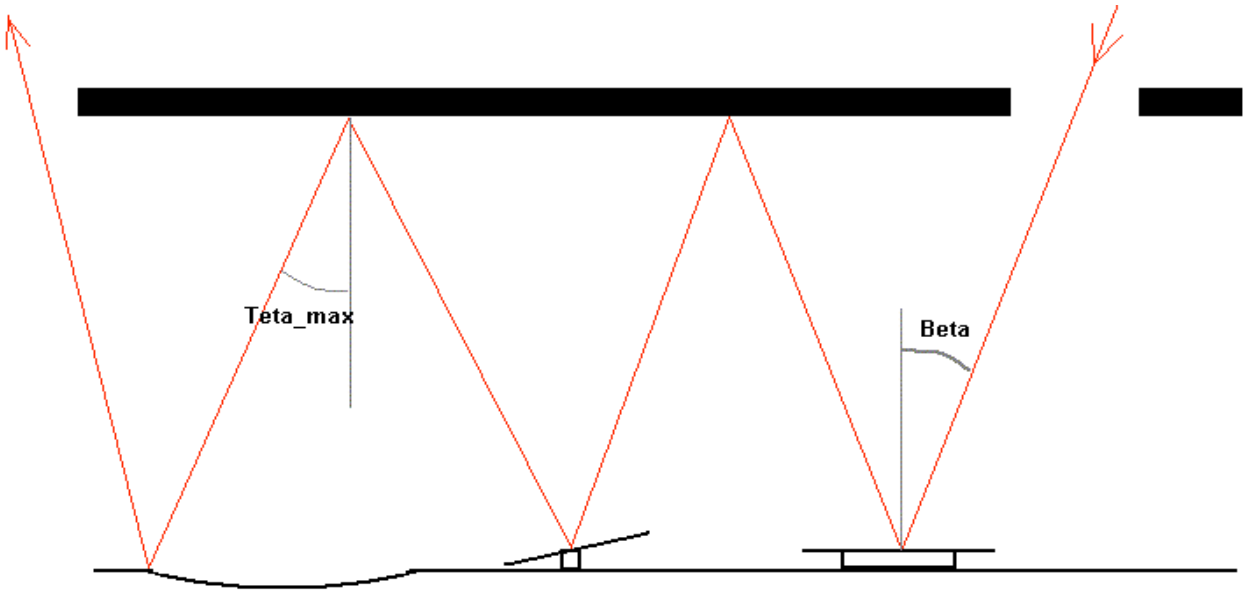

axis of rotation  

We will use OSLO in order to find this angle. The diameter of the aspherical mirror is **505µm**. We optimize here the system with the spot diagram. Indeed, for those angles, the Airy spot (13,5µm) is smaller than the geometric image size.
The focal distance here is 1mm (more or less – see Eugénie Dalimier and Guillaume Lecamp's report).
Here the simulations correspond to a collimated beam which covers all the surface of the mirror but in reality, the diameter of the beam is 100µm only. Thus, if the conic constant we will calculate for each field will be acceptable, the spot size (calculated here) does not correspond to the reality. Nevertheless, it can give us an idea of the quality of the system.
For each angle θmax, we modify the conic constant :

Example of spot diagram (field : 11°)

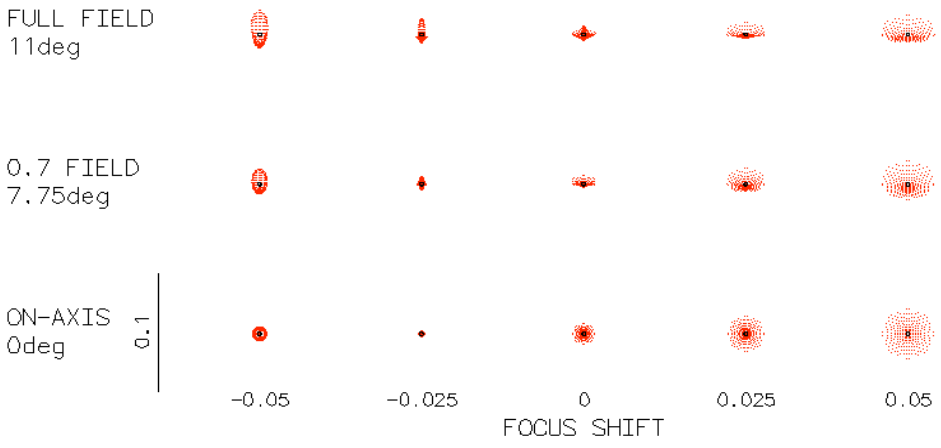

We can sum up the results in a table :

field (°)	Conic Constant	spot size (µm)	Airy spot size
10	4,5	15	13,5 µm
11	5,5	19	
13	6,5	24	
15	8	33	
16	9	35	
18	11,5	40	
20	13,25	45	

If we analyse these results, we can say that the field (θmax) must be less than 15°.
Indeed, if we increase these 15°, the aberrations are no more negligible.
Furthermore, we cannot have a better resolution than 13,5µm. Thus, the minimum θmax will be 10° more or less.
When we have those figures, we can give the other dimensions :

First, we have to notice that the angle θmax is obtained when the galvanometric mirror is repulsed and when the resonant mirror has not moved.

Position of the spot (case : θfinal = θmax) :

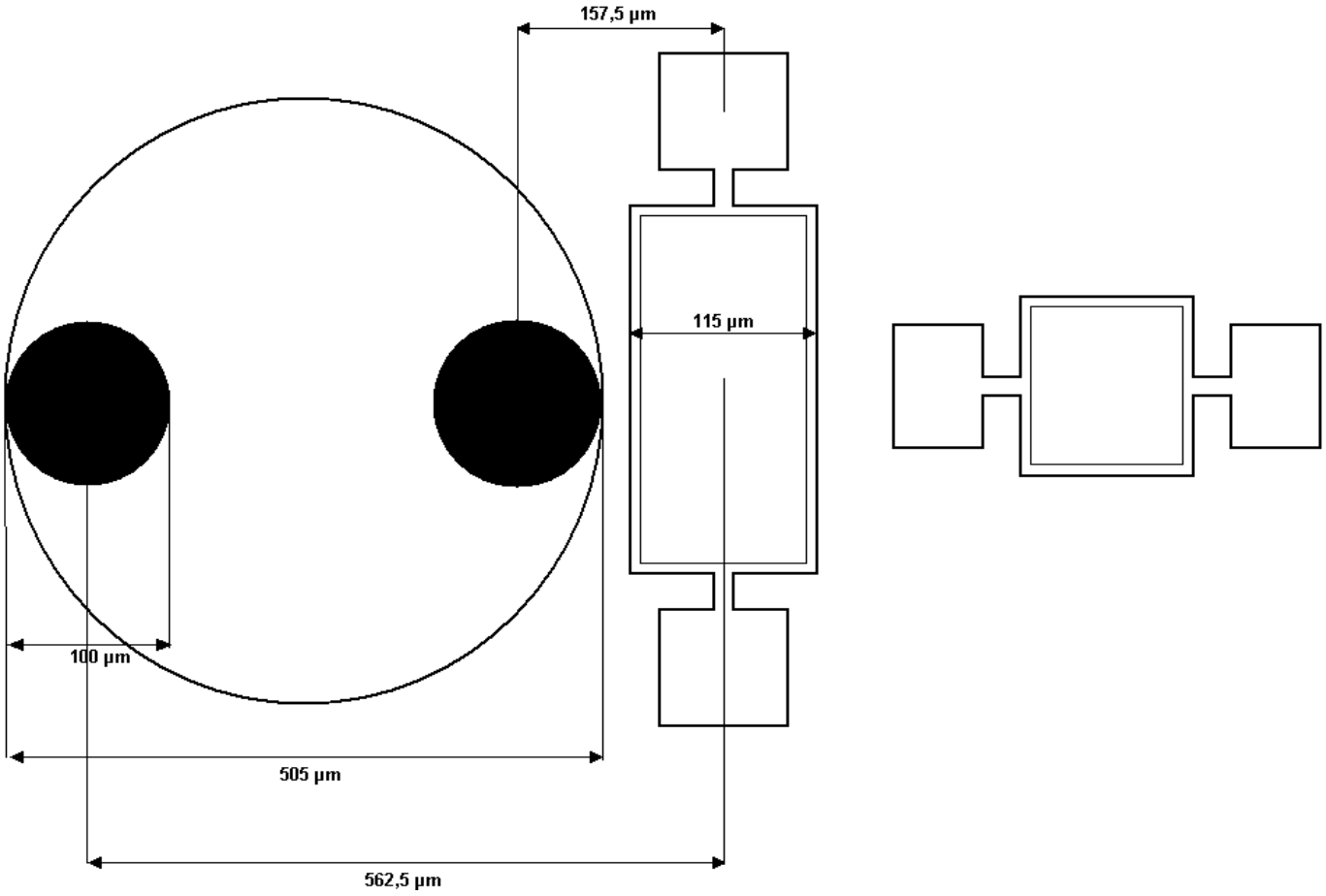

If we consider that the galvanometric mirror width is 115µm (that is to say a little more than the diameter of the beam in order to avoid diffraction from the edges of the micromirror) we have :

$$h = \frac{562,5}{2.\tan(\theta \max)}$$

Then we have θmin which corresponds to the minimum incident angle on the aspherical micromirror (obtained when the galvanometric mirror move on the other side and when the resonant mirror does not move) :

$$\theta\min = \tan^{-1}(157,5/(2.h))$$

Thus we have the optical scan angle (for the beam) in the vertical direction :

$$\Delta\theta = \theta\max - \theta\min$$

Then, we can calculate the rotations of the galvanometric micromirror (α_{max} for θ_{max} and α_{min} for θ_{min}).
But α_{max} and α_{min} are a function of the distance D between the two movable micromirrors. We can make another hypothesis : $|\alpha_{max}| = |\alpha_{min}| = \alpha$. In this way, we minimize the rotation of the micromirror. Indeed if we have $|\alpha_{max}| \neq |\alpha_{min}|$, we must have $|\alpha_{max}| > \alpha$ or $|\alpha_{min}| > \alpha$.

If β is the angle at the beginning, we have :

$\alpha_{min} = (\theta_{min} - \beta) / 2$ **(1)** and $\alpha_{max} = (\theta_{max} - \beta) / 2$ **(2)**
$\alpha_{min} = -\alpha_{max}$ => $\beta - \theta_{max} = \theta_{min} - \beta$ and thus :

$$\beta = \frac{\theta \max + \theta \min}{2}$$

And then, thanks to (1) or (2), we have $\alpha_{max} = -\alpha_{min}$

The distance D between the two micromirrors is :

$$D = 2.h.\tan(\beta)$$

Finally, we calculate the rotations of the resonant scanner :

$$\alpha'\max = -\alpha'\min = \alpha' = \tan^{-1}(202,5 / (4.h)) / 2$$

We can group the results in a table :

teta max (°)	h (µm)	teta min (°)	beta (°)	D (µm)	alpha (°)	alpha' (°)
10	1595,05	2,83	6,41	358,57	1,79	0,91
11	1446,91	3,12	7,06	358,27	1,97	1,00
12	1323,18	3,41	7,70	357,94	2,15	1,10
13	1218,23	3,70	8,35	357,58	2,33	1,19
14	1128,03	3,99	9,00	357,19	2,50	1,28
15	1049,64	4,29	9,65	356,77	2,68	1,38

Now, we can discuss about the figures α and α' :

2. Movement of the micromirrors

In fact, we cannot move the mirrors indefinitely because of the depth of the well and because of the deformation of the planar (which is no more planar thus) which is not negligible if the rotation is too important.

Thanks to the software COVENTOR, I have optimized the system and I present in this part the maximum movement of the micromirrors.

The description of this optimization will be described in part III.C.

- *Resonant micromirror*

The deformation of this micromirror is not really a problem. Thus, we chose a 4µm well (thus 5µm between the mirror and the well or else 4µm between the mirror and its electrodes).
The maximum movement is given in the figure below :

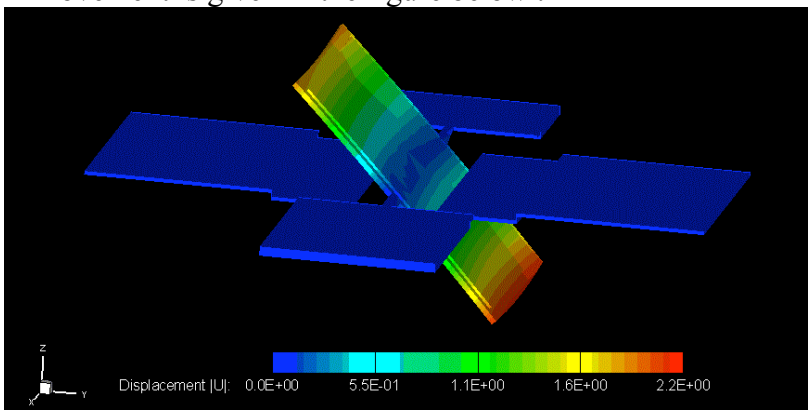

We have exaggerated here the movement : the factor of exaggeration is 30.

The maximum rotation of the mirror is 1,96° = $\alpha_{resonant}$. This figure is higher than all the α' we have calculated : thus, this mirror won't be a predominant limitation and the scan will be possible in all the vertical direction.

- *Galvanometric micromirror*

Here, we prefer using a well which depth is 3µm (that is to say 4µm between the mirror and the SiO_2 or 3µm between the mirror and the electrode) – see part III.C –
The best movement we obtain is given in the figure below :

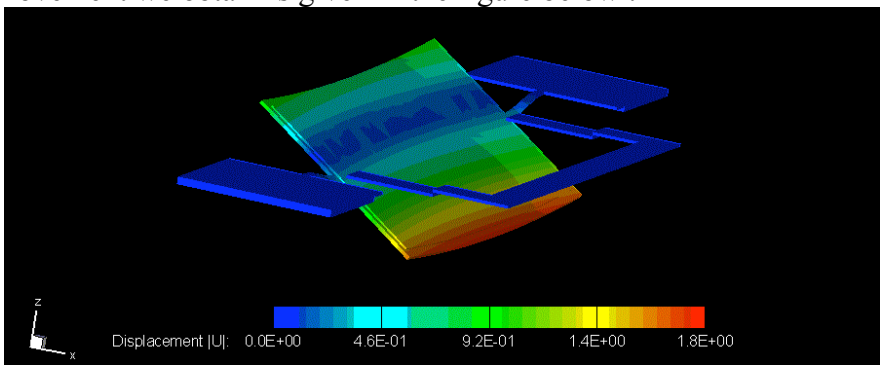

The factor of exaggeration is 30.

The maximum rotation of the mirror is 1,28° = αgalvanometric which is quite small. This is an important limitation for our system.

3. Conclusion concerning the movable micromirrors

We have to find a compromise considering the aberrations and the movement of the galvanometric scanner (the resonant scanner is not a problem). We will choose θmax = 11°. This is an arbitrary choice which correspond to a good resolution.
If we want to make another choice (for θmax, if we want to increase the total scan), we would just have to follow exactly the same calculations which are exhaustively developed in this report.

Thus, we choose :

h = 1445 µm

And thus we have the other dimensions (the precision of the fabrication is 5 µm)

D = 357,5 µm

Indeed, the precision of the fabrication is 5µm, thus, the precision of the position of each center is 2,5µm.

$$\beta = \tan^{-1}\left(\frac{D}{2.h}\right) = 7{,}05°$$

$$\theta\text{min} = \tan^{-1}\left(\frac{157{,}5}{2.h}\right) = 3{,}12°$$

$$\theta\text{max} = \tan^{-1}\left(\frac{562{,}5}{2.h}\right) = 11{,}01°$$

For the galvanometric mirror :

- $\alpha_{min} = (\theta_{min} - \beta) / 2 = -1{,}97°$
- $\alpha_{max} = (\theta_{max} - \beta) / 2 = 1{,}98°$

Thus, we verify here that the rotation of the mirror (1,28°) is smaller than those values.

For the resonant scanner :

- $\alpha' = \tan^{-1}(202{,}5 / (4.h)) / 2 = 1{,}00°$

With this system, we the total optical scan (for the beam that is to say two times the optical scan angle for the mirror) is :
$\Delta\theta = 4*\alpha_{galvanometric\_mirror} = 5{,}12°$ for the horizontal direction
$\Delta\theta' = 4*\alpha' = 4{,}01°$ for the vertical direction

Thus, at the image plane, if the focal distance of the aspherical mirror is **f' = 1,1 mm**, the size of the image scan is :

- $f'*(\tan(\beta+2*\alpha_{galvanometric}) - \tan(\beta-2*\alpha_{galvanometric})) \approx 100$ µm in the horizontal direction

- f'* (2*tan (2*α')) ≈ 77 µm in the vertical direction

These values have to be compared to the Airy spot size (13,5µm) if we consider that we are limited by the diffraction.
We cannot increase really the horizontal scan because it is limited by the movement of the galvanometric micromirror. Nevertheless, we can increase the vertical scan because α' is much smaller than $\alpha_{resonant}$.

Furthermore, all these values are a consequence of an arbitrary choice : θmax = 11°. But this angle is not reached because of the limited movement of the galvanometric micromirror. Thus, we can decrease h in order to increase the scan (and we can suppose that the resolution won't be worse).

We can give the different scan angles (function of h) in a table which gives all the possibilities until $\alpha' \approx \alpha_{resonant}$ (at this moment, we use all the possibilities of the resonant micromirror) :

teta max (°)	h (µm)	teta min (°)	beta (°)	D (µm)	alpha (°)	alpha' (°)	horizontal max	horizontal min	vertical max	vertical min
10	1595,05	2,83	6,41	358,57	1,79	0,91	8,97	3,85	1,82	-1,82
11	1446,91	3,12	7,06	358,27	1,97	1,00	9,62	4,50	2,00	-2,00
12	1323,18	3,41	7,70	357,94	2,15	1,10	10,26	5,14	2,19	-2,19
13	**1218,23**	**3,70**	**8,35**	**357,58**	**2,33**	**1,19**	**10,91**	**5,79**	**2,38**	**-2,38**
14	1128,03	3,99	9,00	357,19	2,50	1,28	11,56	6,44	2,57	-2,57
15	1049,64	4,29	9,65	356,77	2,68	1,38	12,21	7,09	2,76	-2,76
16	980,84	4,59	10,30	356,33	2,85	1,48	12,86	7,74	2,95	-2,95
17	919,93	4,89	10,95	355,85	3,03	1,57	13,51	8,39	3,15	-3,15
18	865,60	5,20	11,60	355,34	3,20	1,67	14,16	9,04	3,35	-3,35
19	816,81	5,51	12,25	354,80	3,37	1,77	14,81	9,69	3,55	-3,55
20	772,73	5,82	12,91	354,23	3,55	1,87	15,47	10,35	3,75	-3,75
21	732,68	6,13	13,57	353,62	3,72	***1,98***	16,13	11,01	3,95	-3,95

We can see that for θmax ≈ 13°, the maximum optical scan is (more or less) 11° (horizontal max).

Thus, we can choose h < 1220µm (the resolution will be limited by diffraction).

With **h = 1220 µm** and **D = 357,5** we have :

$$\beta = 8,34°$$
$$\theta_{horizontal\_max} = \beta + 2*1,28° = 10,90°$$
$$\theta_{horizontal\_min} = \beta - 2*1,28° = 5,78°$$
$$\theta_{verticalmax} = -\theta_{vertical\ min} = 2*\alpha' = 2,38°$$

Thus, at the image plane, we have (with **f' = 1,1 mm**) :

- f'* (tan (β+2*$\alpha_{galvanometric}$) – tan (β-2*$\alpha_{galvanometric}$)) = 100,5 µm in the horizontal direction
- f'* (2*tan (2*α')) = 91,4 µm in the vertical direction

We can increase of course the size of this scan (all the calculations are given in this report) but we do not forget that if we increase this size, $\theta_{horizontal\_max}$ will increase too and thus, there will be aberrations (and thus, the resolution will be worse).

4. The aspherical micromirror.

When we know h, we know the optical scan and especially the maximum scan angle. When we have this maximum angle, we can make a simulation with OSLO in order to find the conic constant of the aspherical micromirror. The results that I have reported below were found with a collimated beam which covered all the surface of the micromirror. But in reality, the size of the beam is only 100 µm and thus, the aberrations are not the same. Nevertheless, we can suppose that the conic constant which is given here corresponds to the best surface :

teta max (°)	Conic Constant
10	-4,5
11	-5,5
12	-6
13	-6,5
14	-7,25
15	-8
16	-9
18	-11,5
20	-13,25

Then, we can fabricate the aspherical micromirror (see part I.B.1).
I have not worked on this fabrication. This work was made by Armando.

C) Movement of the micromirrors

In this part, I will describe the micromirrors themselves. More precisely, I will focus on the dimensions of the different parts of the micromirrors (the arms, the electrode, the well, the mirror itself…) ; indeed, those dimension are responsible of many important things like the rotation angle of the mirrors, the deformation of the mirror when it moves or the voltages we have to impose in order to move the mirrors.

I have optimized the two movable micromirrors with COVENTORWARE.
I will give a brief presentation of this software and then, I will give the optimisation of the two micromirrors I have made.

1. CoventorWare

The first step of the software consists in giving the process of fabrication. But at the end of the process, when we remove the PSG (see part III.A.1), the software considers that all the PSG is removed. Thus, we have to make a little modification in order to simulate the PSG which remains at the end of the process : we introduce a new layer of polysilicon (POLY 3). The new process is given below :

ProcessEditor: D:\Coventor\CoventorUsers\jmr\MirrorDesign\Devices\Espejo_Resonante.proc

File Edit View Help

Step	Action	Type	Layer Name	Material	Thickn...	Color	Mask Name/ Polarity	Depth	Offset	Sidewall Angle
0	Base		Substrate	SILICON	1.0	blue	GND			
1	Deposit	Stacked	Substra...	SILICON	5.0	yello...				
2	Etch	Front, Partial				yello...	Pozo -	4.0	0.0	0.0
3	Deposit	Conformal	SiO2	THERM_OXIDE	1.0 S...	gold				
4	Deposit	Conformal	Poly1	POLYSILICON	2.0	red				
5	Etch	Front, Last L...				red	Poly1 +	2.0	0.0	0.0
6	Deposit	Planar	Via	PSG	1.0	white				
7	Etch	Front, Last L...				white	Via -	1.0	0.0	0.0
8	Deposit	Planar	Poly3	POLYSILICON	1.0	cyan				
9	Etch	Front, Last L...				cyan	Poly3 +	1.0	0.0	0.0
10	Deposit	Planar	Poly2	POLYSILICON	1.0	green				
11	Etch	Front, Last L...				green	Poly2 +	1.0	0.0	0.0
12	Deposit	Planar	Aluminio	ALUMINUM	1.0	light...				
13	Etch	Front, Last L...				light...	Aluminio +	1.0	0.0	0.0
14	Sacrifice			PSG						

The size of the well (« pozo ») is 4µm. This is true for the resonant scanner but the well of the galvanometric mirror is a 3µm well.

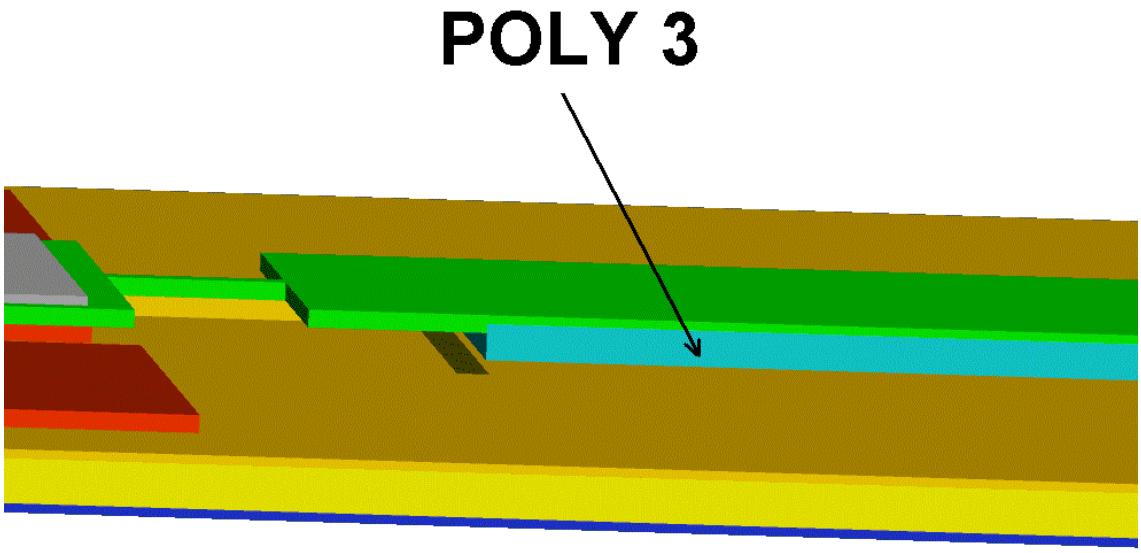

In this step, we give the different thicknesses of the layers (and the depth of each etching).

Then, we define the masks which will be use during the etching of each layer :

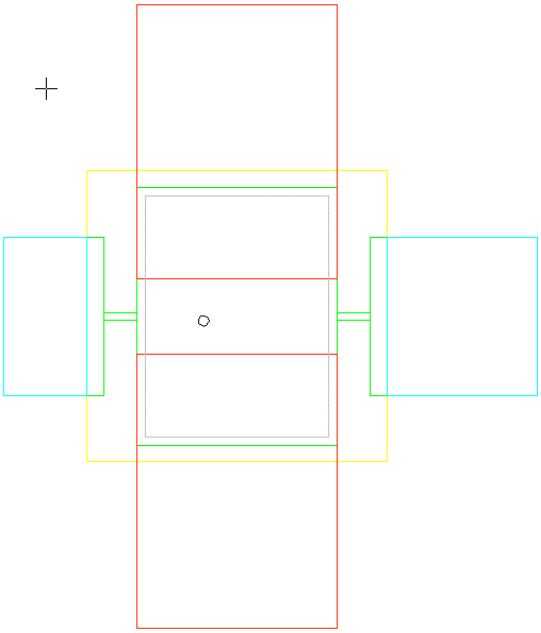

Then, we have a 3-D view of the system and we will mesh the interesting surfaces of the micromirror – see the figure below -(this will make the calculations possible) and we define the physical properties of the material.
Meshing :

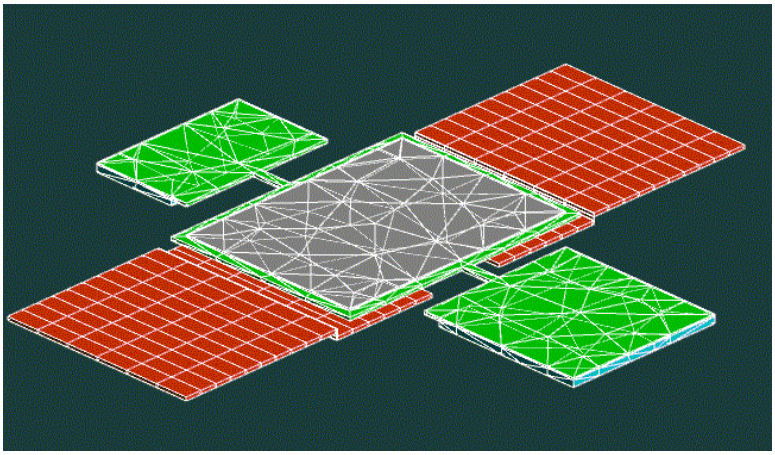

Then, we can simulate : the simulation is a combination between an electrostatic study and a mechanical study. Coventor can give us for example the displacement of the micromirror and a 3-D view of this mirror when it moves (we can see its deformation).

All the photos (of the results) are given with a factor of exaggeration (in order to see better the movement or the deformations).

2. The resonant micromirror

We will try to optimize this first mirror in order to have a reasonable movement without deformation.

- *Theoretical solution*

A 4µm well is necessary if we want to have a reasonable movement

The first thing that needs to be said is that the width of the arms has to be quite little. Indeed, if we do not care about this dimension, the deformation of the mirror during the movement will be catastrophic (see figure below):

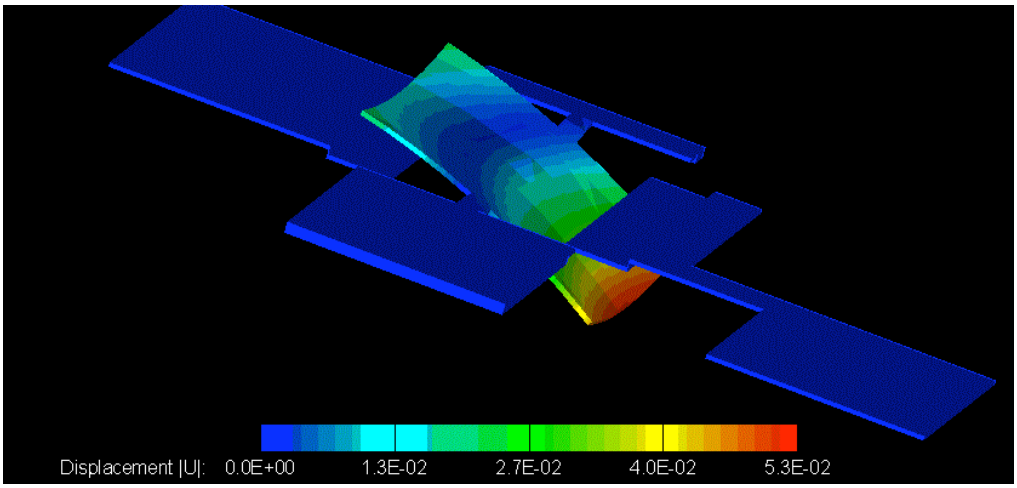

system A : Thickness of the arms : 10 µm

If we reduce this dimension, we can obtain a good movement without deformation :

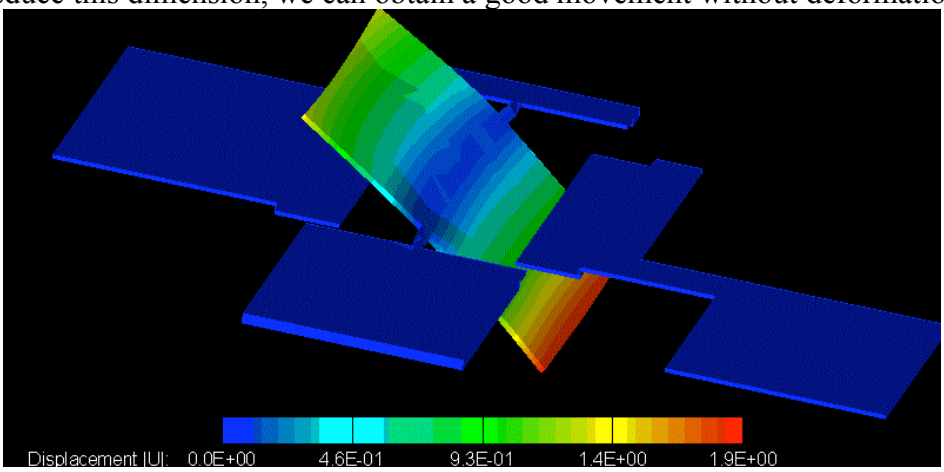

system B : Thickness of the arms : 4µm

Here the mirror stays more planar when it moves. We have not considered in this simulation the layer of aluminium : with this layer, we can say that the deformation is negligible.

We could imagine a mirror with one electrode only :

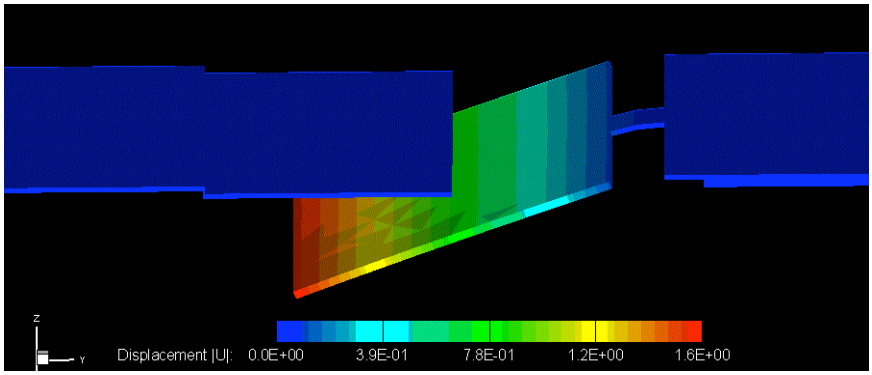

system C : only one electrode

The advantage is that we can place this mirror very close to the galvanometric one (we have to respect a distance of 40µm between two layers which have different voltages).

The inconvenient (much more important) concerns the rotation : for the same displacement (1,6 – 1,9 µm), the angle of rotation is nearly 2 times smaller (because the axis of rotation is different).

Thus we won't accept this solution : the solution (B) seems better.

- *Practical solution*

In practice, it is not possible to have a precision of 4µm for the arms. Indeed, the CMOS technology used at INAOE allows a precision of 5µm (and 1µm for the etch depth or the thicknesses of the layers).

Thus, we will choose arms whose width is 5µm :

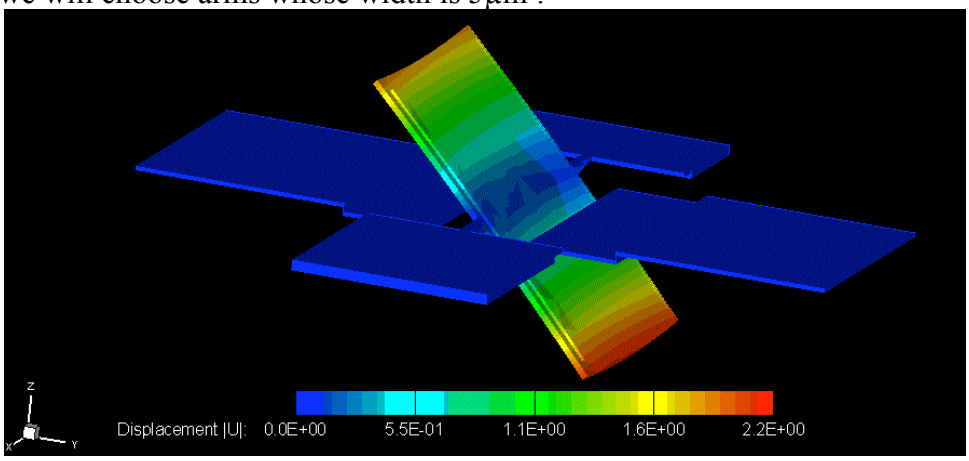

system D : thickness of the arms : 5µm, length of the mirror : 115µm

Nevertheless, the voltage used here is quite high (240 V). We have considered here the layer of aluminium.
We have used here only one electrode for this movement, maybe the voltage will decrease if we use the two electrodes (but I did not succeed in simulating repulsion between two layers with COVENTORWARE).
Another solution could be increasing the length of the mirror :

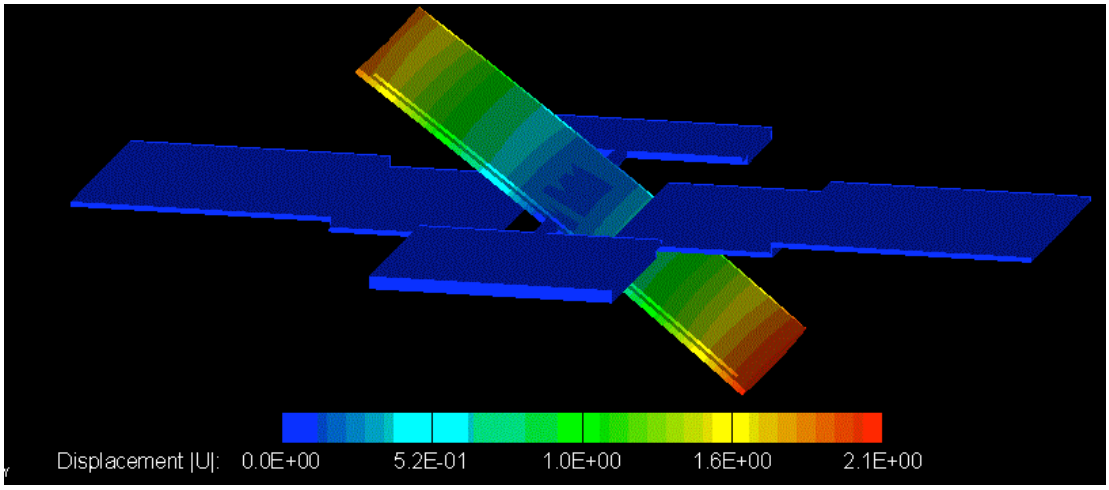

system E : length of the mirror : 155µm

The voltage has been reduced (150 V) and the deformation is quite good too. But an inconvenient is the rotation of the mirror which is smaller for the same vertical displacement of an extremity of the mirror.
Indeed, the maximum rotation of the system D is 1,96° more or less against 1,42° for the system E. But 1,42° is sufficient if h > 1045 (see part III.B.3).

This is the system we will choose.

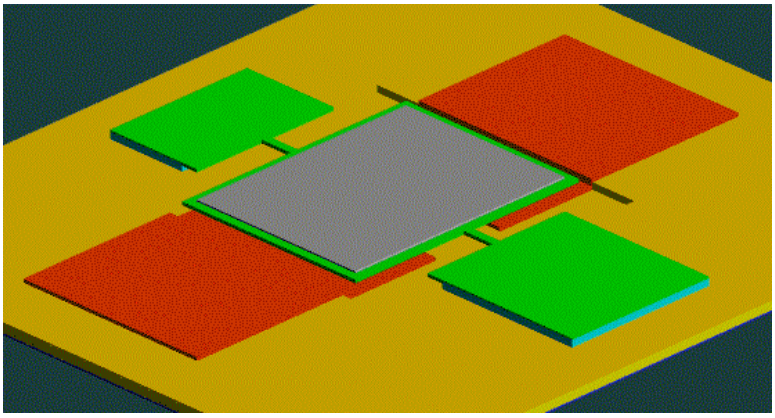

We can give its characteristics :

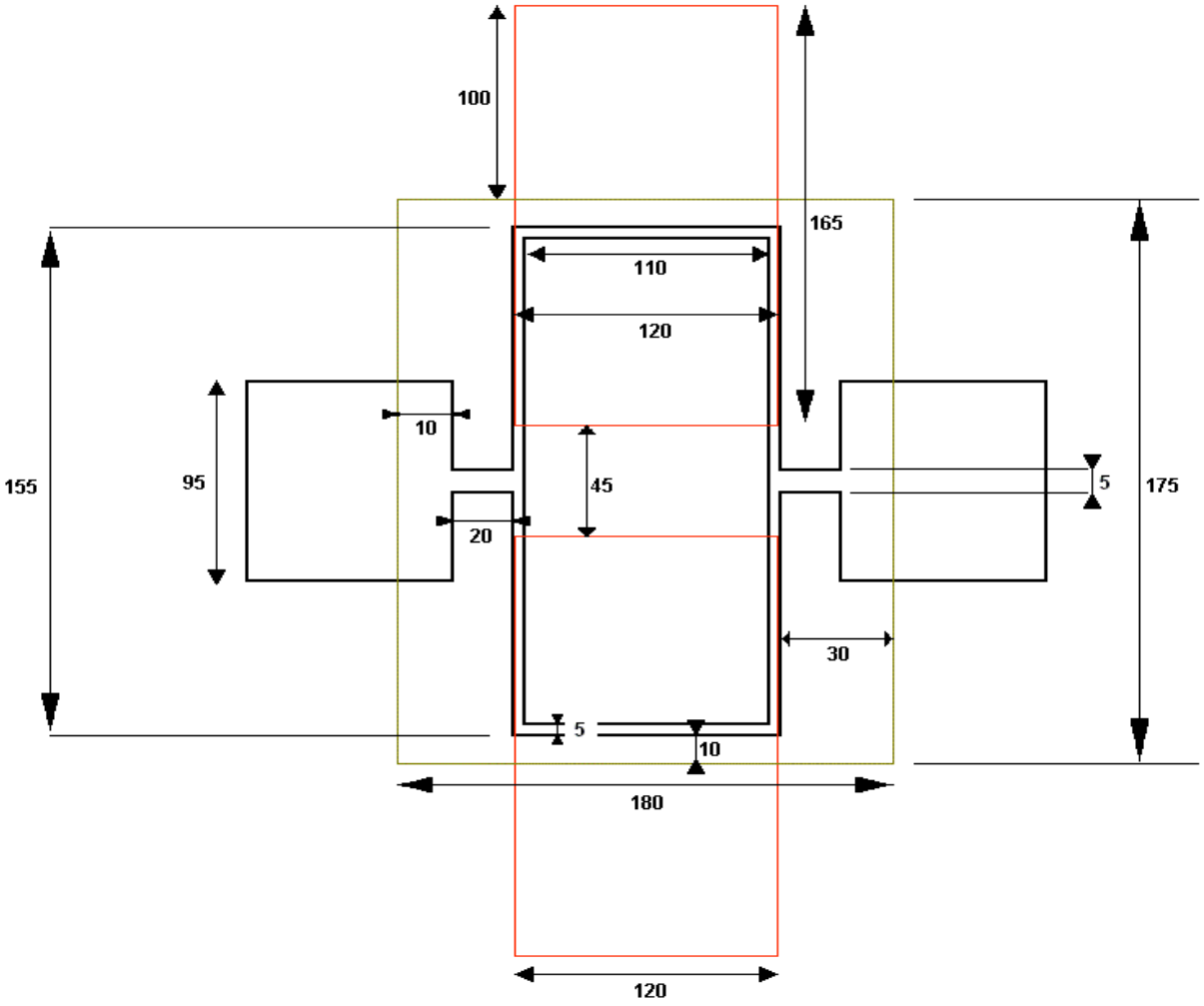

(these values are given in micrometers)

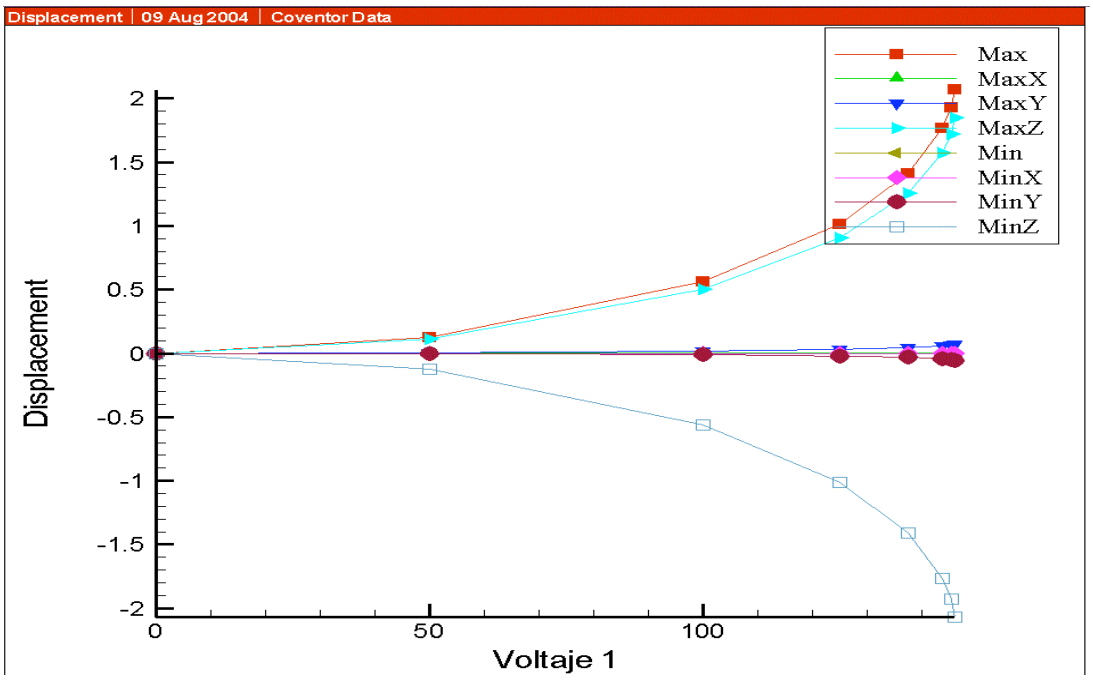

3. The galvanometric micromirror

The width of the mirror must be higher than 100µm (the diameter of the beam is less than 100 µm – or equal – and in this way, we avoid diffraction). We choose here 105µm for this width. The length of the mirror has to be large enough when the vertical scan (which corresponds to the resonant scanner movement) is at its maximum. 330µm is the length we choose for this mirror.

The optimization of the galvanometric micromirror is more difficult because of its higher size (especially the 330µm-length). Indeed, when this mirror moves, there is a great problem of deformation. Thus, the movement of this mirror will be smaller than for the resonant mirror and thus, the size of the well will be smaller too (4µm in theory – it was the same for the resonant scanner – but 3µm in practice).

- *Theoretical solution*

Of course, if the width of the arms cannot be large (problems of deformation). We can observe it with the system below :

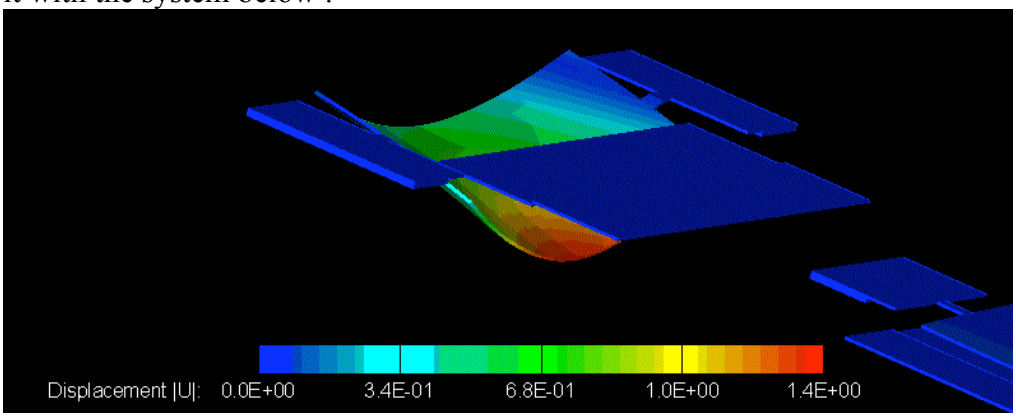

system F : thickness of the arms : 10 µm

This is the worst result of my work !

The thickness of the arms is quite important here. We can make a “hole” in the electrode too : in this way, the force will be applied on the edges of the mirror and not on the center (and thus, the deformation will be more acceptable).
The photos below show the importance of the thickness of the arms. The width of the arms in system G is 4µm against 2µm for the system H :

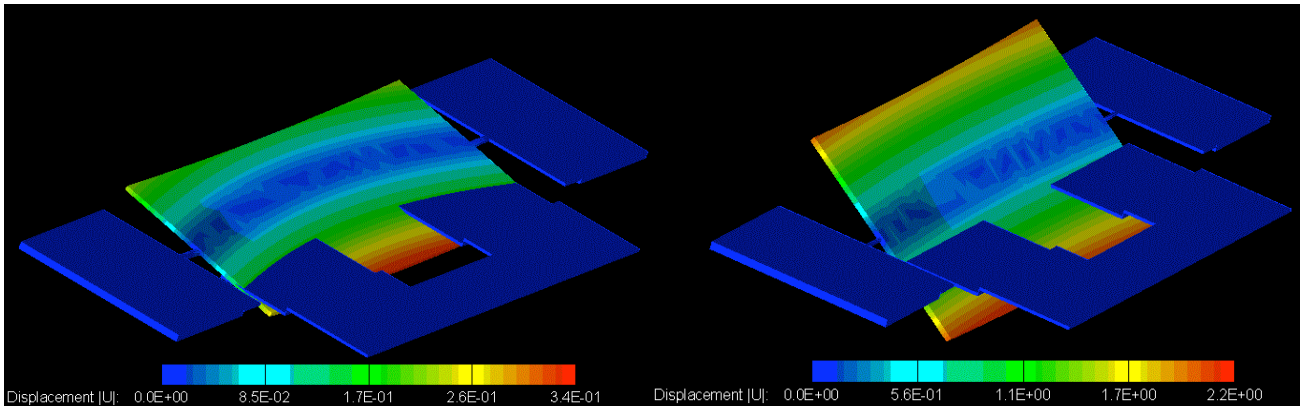

system G system H

We can compare too the system H with the same system without the hole in the electrode (system I):

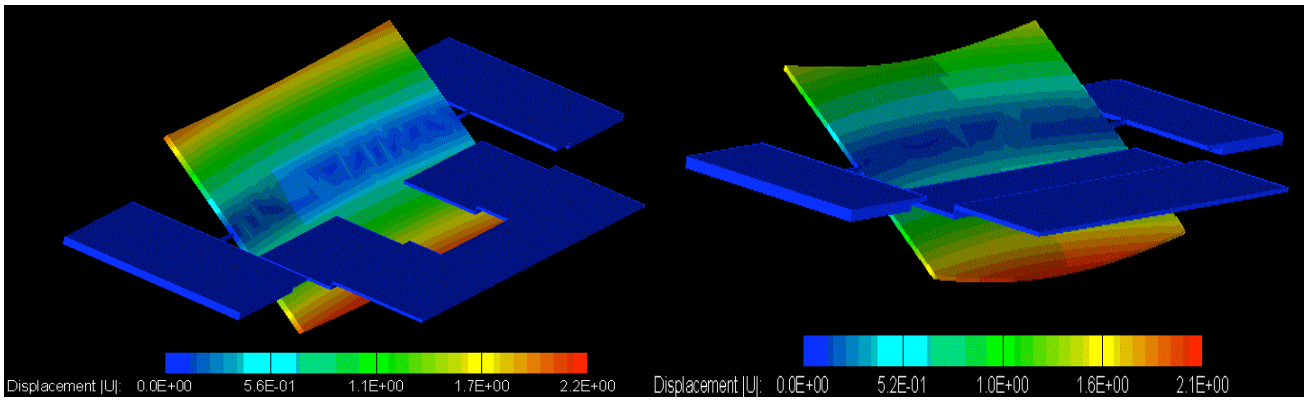

system H system I

Thus, if the voltage is lower for the system I (50 V against 62V for the system H), the deformation is a problem and it can be concluded that the hole in the electrode is not negligible.

As a conclusion, we can say that we have found a good theoretical solution with the system H. Furthermore, the well of the system H is 4µm : we have in this case a good movement without important deformations. But as for the resonant scanner, the technology CMOS we use allows a precision of 5µm. Thus, we have to find another practical solution with arms whose width is 5µm.

- *Practical solution*

We are limited by 5µm arms but we can increase the size of the hole in the electrode. Thus, we can consider the system H with 5µm-arms and we increase the size of the hole. We obtain sensitive improvements with a 285µm-hole (system J) :

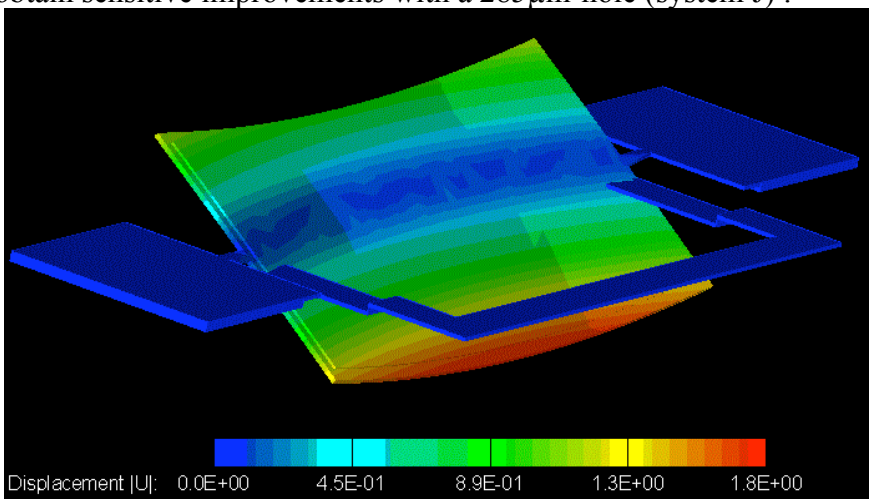

system J (size of the well : 4µm)

But the problem here concerns the voltages. Here, in this movement was possible with 300 V (it would be less with a 3µm-well but it would be high too). We can decrease this voltage increasing the length of the arms.
In the system J, the length of the arms is 20µm and we increase it in the systems K (40µm arms), L (60µm). In those systems, the size of the well is 3µm:

System K (maximum voltage : 150V) :

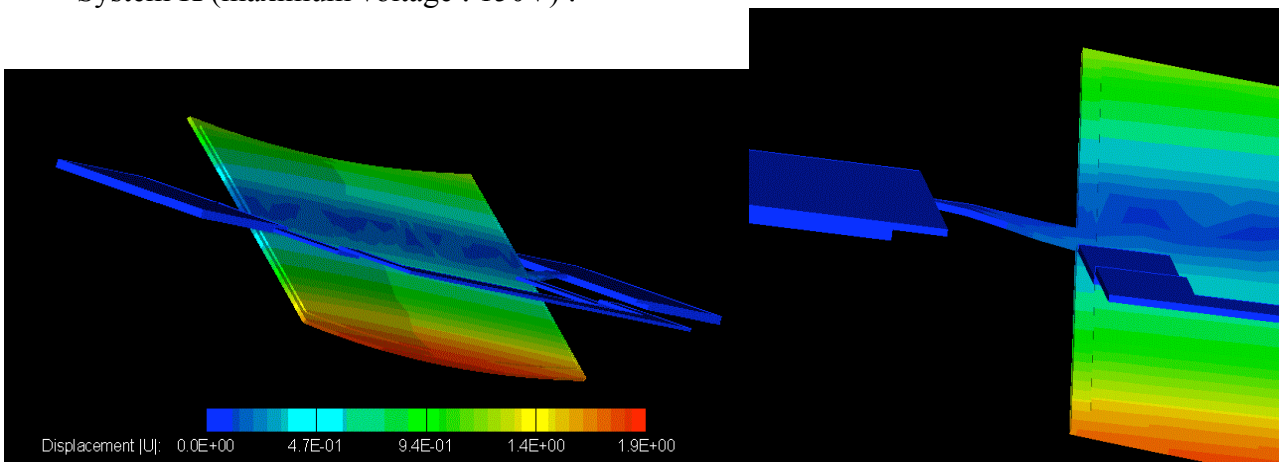

System L (maximum voltage : 115V) :

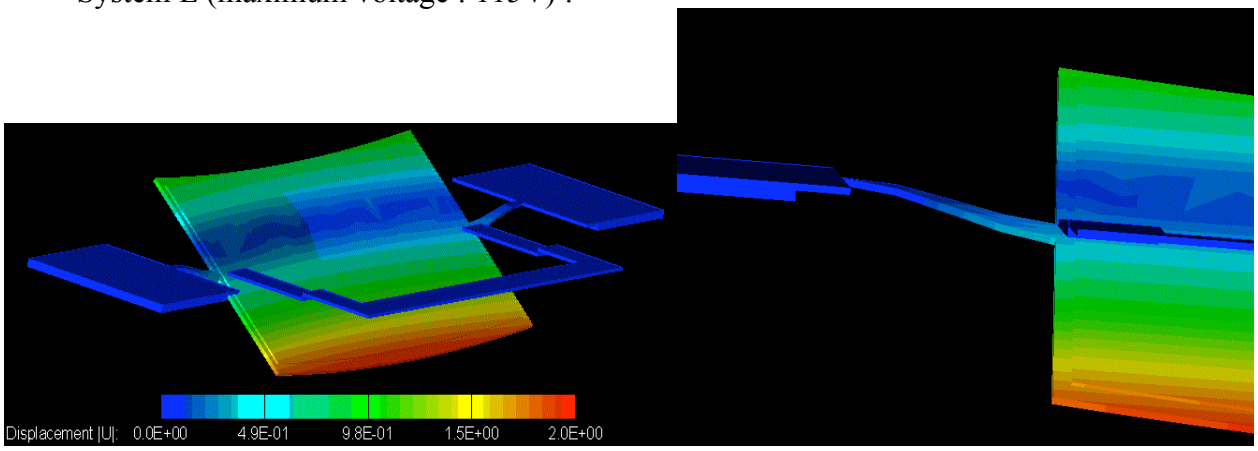

If we still increase the length of the arms, there will be an important problem of depression. Thus, the length of the arms should be between 40 and 60 µm. We will prefer the **40µm** solution because of this problem of depression which is less than if we use 60µm-arms but this solution (with 60µm arms) is good too (and its voltage of 115V could be another criteria) : this choice is an arbitrary one.

The characteristics of our practical solution are given below :

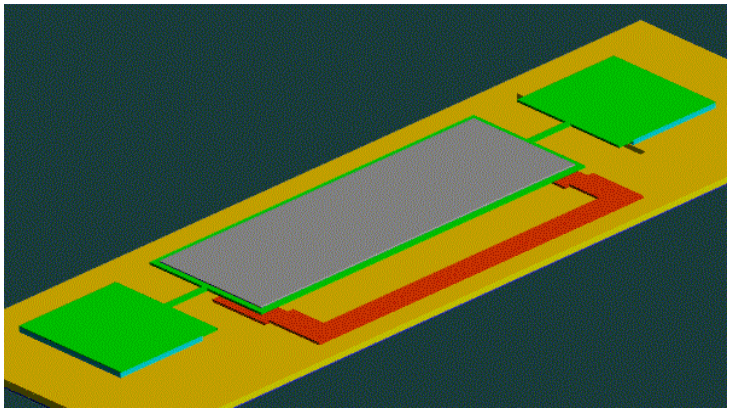

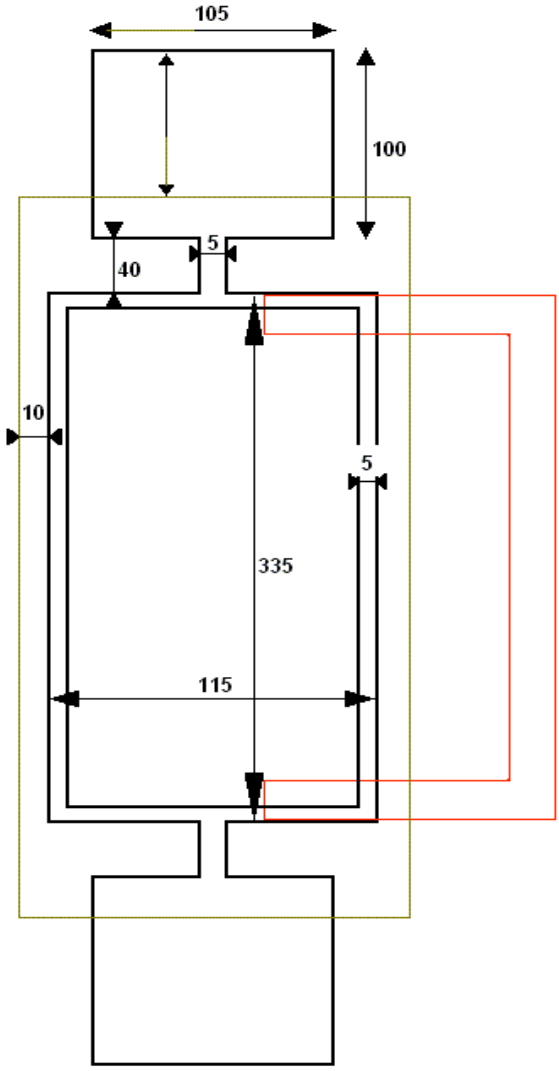

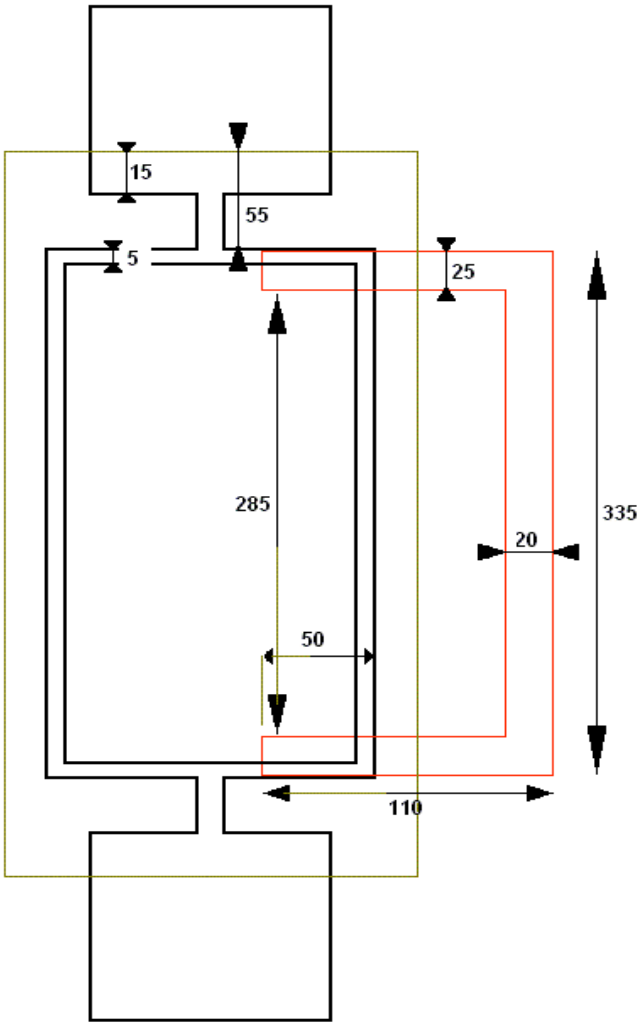

(these values are given in micrometers).

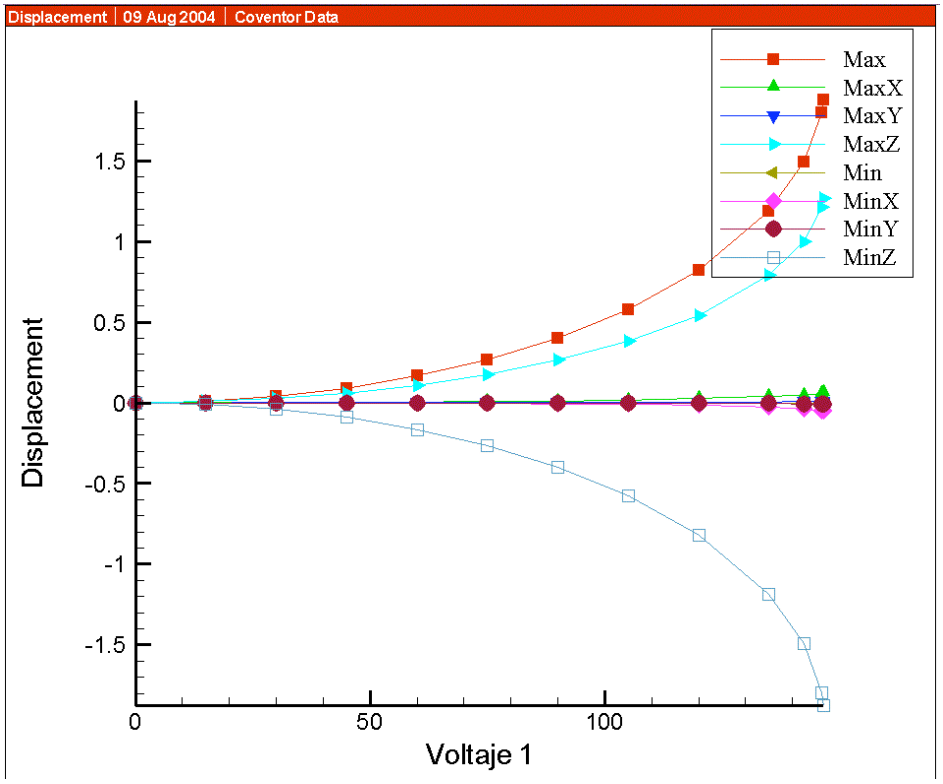
Displacement | 09 Aug 2004 | Coventor Data
Max
MaxX
MaxY
MaxZ
Min
MinX
MinY
MinZ
Displacement
1.5
1
0.5
0
-0.5
-1
-1.5
0
50
100
Voltaje 1

Conclusion:

We have thought and optimized a 2D-scanner which uses two micromirrors. It would be interesting to fabricate concretely this system and of course to test it in order to verify the simulations.

The optical scan of our system is much less than the optical scan of the microscanners we have described in part II. Nevertheless, we can consider that the resolution of our system is very good (in some cases, our system can be considered as limited by diffraction).

We could add a system after this one in order to increase the total scan angle. What's more, we have not studied the resonance of the micromirrors. If we use the magnitude amplification at the resonance, we could imagine that the movement of the mirrors would be amplified and that the voltages would decrease.

We can copy this system too and reproduce it several times in order to make an array of microscanners : this is a way of increasing the total scan image.

Finally, it remains two last steps (concerning the design of this microscanner) : indeed, it would be interesting to propose a packaging and characterizations standards for this system.

Vocabulary:

MEMS : Micro-Electro-Mechanical Systems

MOEMS : Micro-Opto-Electro-Mechanical Systems

Etch rate : The etch rate R_{pqr} gives the speed of the etching of the silicon in the direction <pqr> (in Å/min).

Etch ratio : The etch ratio is the ratio between two etch rate (for example $m=R_{pqr}/R_{p'q'r'}$)

Sagitta : The sagitta (s) is the distance between the "uppest point" of a mirror and the lowest one :

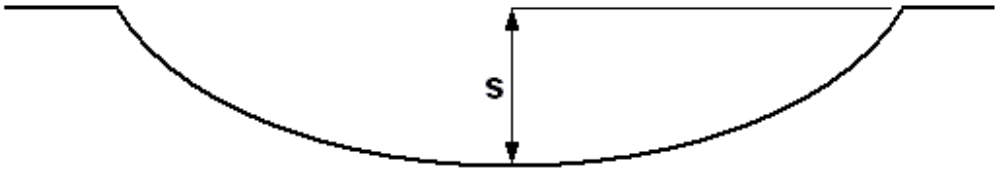

Bibliography:

http://courses.washington.edu/mengr599/tm_taya/notes/c1.pdf

http://www.laas.fr/~bestibal/Biblio/PDF/CAO-Texte-TP.pdf

http://www.dbanks.demon.co.uk/ueng/surfum.html

D.W. de Lima Monteiro, O. Akhzar-Mehr, P.M. Sarro and G.Vdovin, "*Single-mask microfabrication of aspherical optics using KOH anisotropic etching of Si"*, 8 September 2003 / Vol.11 No.18 / Optics Express 2244

Kenneth E. Bean, *Anisotropic Etching of Silicon,* IEEE transactions on electron devices, Vol. ED-25, No 10, October 1978, p.1185-1192

Ernest Bassous, *Fabrication of Novel Three-Dimensional Microstructures by the Anisotropic Etching of (100) and (110) Silicon,* IEEE transactions on electron devices, Vol.ED-25, No 10, October 1978, p1178 – 1184

Meng-Hsiung Kiang, Olav Solgaard, Richard S. Muller, Kam Y.Lau, *Micromachined microscanners for optical scanning,* SPIE Vol.3008, p.82-90

Meng-Hsiung Kiang, Olav Solgaard, Richard S. Muller, Kam Y.Lau, *Micromachined Polysilicon Microscanners for Barcode Readers,* IEEE Photonics Technology Letters, Vol.8, No12, December 1996, p.1707-1709

Meng-Hsiung Kiang, Olav Solgaard, Richard S. Muller, Kam Y.Lau, *Polysilicon optical microscanners for laser scanning displays,* Sensors and Actuators A 70, 1998, p.195-199

D.A. Francis, M.-H. Kiang, O. Solgaard, K.Y. Lau, R.S. Muller and C.J. Chang-Hasnain, *Compact 2D laser beam scanner with fan laser array and Si micromachined microscanner,* Electronic Letters, Vol.33, No.13, IEE, p.1143-1145, 19 June 1997